QUANTITATIVE FINANCE
RESEARCH CENTRE

UNIVERSITY OF
TECHNOLOGY SYDNEY

THINK.CHANGE.DO

QUANTITATIVE FINANCE RESEARCH CENTRE

Research Paper 322 December 2012

The Affine Nature of Aggregate Wealth Dynamics

Eckhard Platen and Renata Rendek

ISSN 1441-8010 www.qfrc.uts.edu.au

The Affine Nature of Aggregate Wealth Dynamics

Eckhard Platen [1] and **Renata Rendek** [2]

December 19, 2012

Abstract: The paper derives a parsimonious two-component affine diffusion model for a world stock index to capture the dynamics of aggregate wealth. The observable state variables of the model are the normalized index and the inverse of the stochastic market activity, both modeled as square root processes. The square root process in market activity time for the normalized aggregate wealth emerges from the affine nature of aggregate wealth dynamics, which will be derived under basic assumptions and does not contain any parameters that have to be estimated. The proposed model employs only three well interpretable structural parameters, which determine the market activity dynamics, and three initial parameters. It is driven by the continuous, nondiversifiable uncertainty of the market and no other source of uncertainty. The model, to be valid over long time periods, needs to be formulated in a general financial modeling framework beyond the classical no-arbitrage paradigm. It reproduces a list of major stylized empirical facts, including Student-t distributed log-returns and typical volatility properties. Robust methods for fitting and simulating this model are demonstrated.

JEL Classification: G10, C10, C15
1991 *Mathematics Subject Classification:* 62P05, 62P20, 62G05, 62-07, 68U20

Key words and phrases: Aggregate wealth dynamics, nondiversifiable market risk, market activity, stochastic volatility, square root processes, benchmark approach.

---

[1] University of Technology Sydney, Finance Discipline Group and School of Mathematical Sciences, PO Box 123, Broadway, NSW, 2007, Australia, Email: Eckhard.Platen@uts.edu.au, Phone: +61295147759, Fax: +61295147711.

[2] University of Technology Sydney, School of Mathematical Sciences, PO Box 123, Broadway, NSW, 2007, Australia, Email: Renata.Rendek@uts.edu.au, Phone: +61295147781.

1 Introduction

This paper models the dynamics of aggregate wealth, more precisely, the dynamics of a world stock index in different currency denominations. Based on first principles, it explains the potential nature of normalized aggregate wealth dynamics as that of a time transformed square root process $Y = \{Y_\tau, \tau \geq 0\}$, satisfying in some market activity time τ the stochastic differential equation

$$dY_\tau = (1 - Y_\tau)d\tau + \sqrt{Y_\tau}dW(\tau), \tag{1.1}$$

where $W(\tau)$ follows a Brownian motion in τ-time, modeling the continuous nondiversifiable uncertainty. Additionally, a market activity time τ_t exaggerates the movements of the resulting volatility, reflecting the impact of typical human behavior a market activity. The two components of the model are the normalized index and the inverse of market activity. Both are modeled as square root processes, where the first one is moving slower than the second one. Both are only driven by the nondiversifiable uncertainty of the market. To be valid over long periods of time for a world stock index, the model needs to be formulated in a general financial modeling framework beyond the classical no-arbitrage paradigm. The paper will demonstrate that the proposed one-factor, two-component affine diffusion model, with three structural and three initial parameters, reproduces well a list of seven major stylized empirical facts and is difficult to falsify.

The standard continuous market model for an equity index has been the Black-Scholes model, see Black & Scholes (1973) and Merton (1973), which employs the exponential of a time transformed Brownian motion to describe the index dynamics, resulting in its standard version in constant volatility and Gaussian log-returns. Its historical popularity is due to its tractability and simplicity. Several shortcomings of this model became apparent since its introduction. Most striking is the observation that, in reality, the volatility of an equity index is stochastic and its return distribution is leptokurtic.

Streams of literature aiming for improvements on the standard market model by modeling volatility as a stochastic process, include the broad literature on autoregressive conditional heteroscedastic (ARCH) models and its generalizations, initiated by Engle (1982). The reader can find a systematic introduction into the extremely rich literature on continuous time stochastic volatility models, for instance, in Cont (2010). An important class of volatility models has been studied in the literature on local volatility function models; see for instance Dupire (1992) and Derman & Kani (1994b). This popular type of continuous stochastic volatility models generalizes the constant elasticity of variance (CEV) model, which goes back to Cox (1975) and Cox & Ross (1976). We will see that the proposed model will have some similarity to CEV type models, and also to those that employ some random market activity time in the sense of subordination; see Clark (1973) and Bochner (1955).

More recently, Lévy processes and jump diffusion processes have been used in asset price and index modeling, see e.g. Madan & Seneta (1990), Eberlein & Keller (1995), Barndorff-Nielsen & Shephard (2001) and Kou (2002). By modeling a world stock index we face primarily the continuous nondiversifiable uncertainty of the equity market and can, in a first approximation, neglect jumps in this paper.

Despite of several decades of intense research on financial market modeling, no consensus emerged about what constitutes a workable model for equity indices. This paper argues that one major reason for the apparent deadlock is the failure of identifying a suitable object of study that could be modeled in a parsimonious and robust manner. Stock prices and exchange rates should be expected to be driven by at least two sources of uncertainty. These include the uncertainty related to the denominating currency and the one related to the security itself. Disentangling their impact in a parsimonious model represents an important challenge. This paper demonstrates how to overcome the seemingly hopeless situation by studying the dynamics of a world stock index, in the denomination of currencies.

A second major reason for the apparent deadlock is the absence of a theoretical reason that explains the nature of the dynamics of aggregate wealth. The paper conjectures the typical dynamics of aggregate wealth from the limiting dynamics of the sum of the values of many independent economic activities and "projects" over small time periods. In a first approximation, the variance of the increments of aggregate wealth turns theoretically out to be proportional to the number of these activities and "projects". This means that the variance is *proportional* to the aggregate wealth itself. As a consequence, the aggregate wealth itself follows approximately a time transformed square root process. With respect to transformed time the inverse of the square root process is then the resulting squared volatility. A very realistic, parsimonious one-factor, two-component model emerges by modeling the human behavior, which exaggerates the reactions in volatility to ups and downs of the index. These exaggerations are modeled through the transformed time via another (fast moving) square root process.

Note that if the dynamics of a world stock index are modeled in different currency denominations then, an exchange rate can be described as the ratio of two respective currency denominations of the index. Similarly one can model stock prices and commodity prices.

The benchmark approach exploits in this paper the fact that currency denominations of a world stock index have more clearly identifiable empirical properties than, say, an exchange rate. For instance, it is well observed that the average volatility of a currency denomination of a world stock index is smaller than the average volatility of an exchange rate. A world stock index, denominated in a given currency, is primarily driven by the nondiversifiable uncertainty of the market with respect to that currency as denominator. This paper makes this nondiversifiable uncertainty the single driver of the dynamics of the two components in the proposed model for this index denomination. It argues that there is no need for any extra noise source. By systematically comparing a list of seven major stylized empirical facts of the world stock index dynamics in various currency denominations, with the properties of the proposed two-component model, it turns out that the model is difficult to falsify in the sense of Popper (1934), but many other models are rejected. Finally, an almost exact simulation method is described for the model, which allows to generate trajectories over long time periods accurately with typical extreme events and stationary density.

The paper is organized as follows: Section 2 derives the affine nature of aggregate wealth dynamics. Section 3 extracts a list of stylized empirical facts for its dynamics in currency denominations. Section 4 proposes a parsimonious index model involving the power of a time transformed affine diffusion. Section 5 discusses the volatility and market activity dynamics arising from the proposed model. Section 6 places the model in a generalized financial market modeling framework beyond the classical no-arbitrage paradigm. Section 7 describes a robust step-by-step methodology for fitting the proposed model. Section 8 visualizes volatility and market activity as they emerge under the model. As an example for the wider applicability of the proposed model Section 9 fits the S&P500 to the model and compares its theoretically calculated volatility with the volatility index VIX. Section 10 describes for the model an almost exact simulation method, which allows to confirm in Section 11 that the empirical properties of the model match the list of stylized empirical facts.

2 Dynamics of Aggregate Wealth

To obtain an idea what type of stochastic process may be well suited for modeling a normalized world stock index, we ask the question, what would be the type of limiting diffusion process that may likely emerge for the aggregate wealth of an economy? We consider normalized units of wealth such that the long term exponential growth of the economy is taken out on average and some kind of equilibrium may be observed. For simplicity, consider a multi-period discrete time setting, and assume at time $\tau_i = i\Delta, i \in \{0, 1, \dots\}$, $0 < \Delta < 1$, that the economy has accumulated the total wealth $Y^{\Delta}_{\tau_i}$, each wealth unit worth $\sqrt{\Delta}$, $Y^{\Delta}_0 = Y_0 > 0$. This means, one has about $\frac{Y^{\Delta}_{\tau_i}}{\sqrt{\Delta}}$ wealth units at time τ_i. During the period until time $\tau_{i+1} = \tau_i + \Delta$ each wealth unit invests in a "project" or pursues some economic activity, which "consumes" on average $\eta\Delta$ units of wealth, $\eta > 0$. Furthermore, $\beta\sqrt{\Delta}$ new wealth units are generated, on average, during the time period, $\beta > 0$. This means, the mean of the increment of aggregate wealth for the time period equals $(\beta - \eta Y^{\Delta}_{\tau_i})\Delta$.

Most important for understanding the nature of aggregate wealth dynamics is the fact that, in a first approximation, it is appropriate to assume that the outcomes of the "projects" and economic activities are independent of each other. This means, if we assume, for simplicity, that each "project" and economic activity generates in the period $[\tau_i, \tau_{i+1})$ wealth with variance $\upsilon^2 \Delta^{\frac{3}{2}}$, then, the variance of the increment of the aggregate wealth amounts to $\upsilon^2 Y^\Delta_{\tau_i} \Delta$. Obviously, its deviation is then $\upsilon \sqrt{Y^\Delta_{\tau_i} \Delta}$. Note that, very naturally, a square root of aggregate wealth appears in the deviation of aggregate wealth. Note that it does not matter much what type of distribution the individual wealth outcomes have when these are generated by different "projects" or economic activities. Intuitively, by the Central Limit Theorem the increment $Y^\Delta_{\tau_{i+1}} - Y^\Delta_{\tau_i}$ of aggregate wealth is for $\Delta \to 0$ asymptotically conditionally Gaussian distributed with the above mean and variance. Moreover, the difference equation

$$Y^\Delta_{\tau_{i+1}} - Y^\Delta_{\tau_i} = \left(\beta - \eta Y^\Delta_{\tau_i}\right) \Delta + \upsilon \sqrt{Y^\Delta_{\tau_i}} \Delta W_{\tau_i}, \tag{2.1}$$

with ΔW_{τ_i} denoting a random variable approximately with mean zero and variance Δ, resembles an Euler scheme, see Kloeden & Platen (1999), of the square root process $Y = \{Y_\tau, \tau \geq 0\}$ with stochastic differential equation (SDE)

$$dY_\tau = (\beta - \eta Y_\tau)\, d\tau + \upsilon \sqrt{Y_\tau} dW(\tau), \tag{2.2}$$

$\tau \geq 0, Y_0 > 0$. Here $W = \{W(\tau), \tau \in [0, \infty)\}$ is a standard Brownian motion. Along the lines of Alfonsi (2005) and Diop (2003) it follows under rather general assumptions, that for vanishing time step size $\Delta \to 0$ the aggregate wealth process Y^Δ converges in a weak sense, see also Kloeden & Platen (1999), to the affine diffusion process $Y = \{Y_\tau, \tau \in [0, \infty)\}$, satisfying the SDE (2.2). Note that the solution $Y = \{Y_t, t \in [0, \infty)\}$ of the SDE (2.2) is a square root process and, thus, an affine process, see e.g. Duffie & Kan (1994). More precisely, a square root process is sometimes referred to as CIR (Cox, Ingersoll & Ross (1985)) interest rate process. This nonnegative affine process has an explicitly known transition density, see Revuz & Yor (1999).

Most important for the nature of aggregate wealth dynamics is the fact that the diffusion coefficient turns out to be proportional to the square root of the total wealth Y_τ. This is a consequence of the independence of outcomes of "projects" and economic activities. The drift is here in a first approximation and for natural reasons linear in Y_τ, which makes Y a highly tractable affine process.

We know a wide range of important properties of this process. For example, when assuming $\beta > \frac{\upsilon^2}{2}$, the value Y_τ never reaches zero; see Revuz & Yor (1999). Note that the volatility of the limiting aggregate wealth process emerges as $\frac{\upsilon}{\sqrt{Y_\tau}}$. This kind of volatility process models the well-known leverage effect without involving considerations on company value to debt ratios, as e.g. suggested in Black (1976). Under the above approach volatility emerges naturally as a consequence of the uncertain nature of economic activity. The market capitalization weighted index represents, in a first approximation, the aggregate wealth of the economy, which is here modeled.

Economic and market activity change over time. People react to the observed aggregate wealth evolution in their economic activity, including their trading

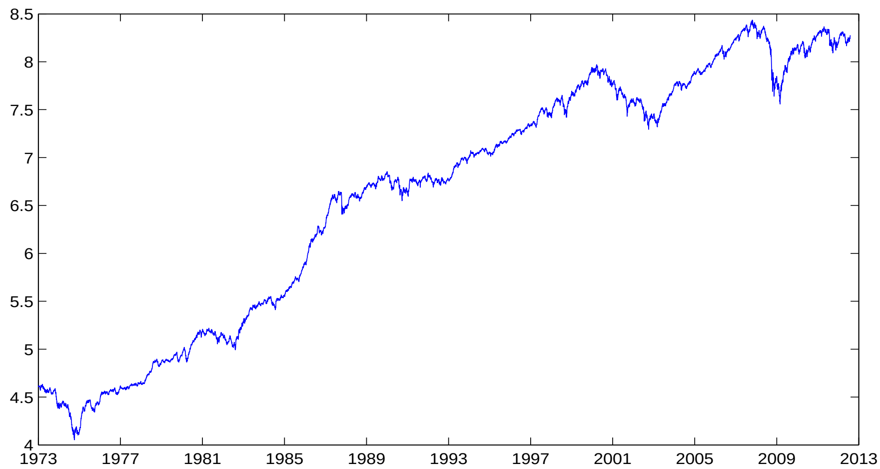

Figure 3.1: Logarithm of a well diversified world stock index MCI.

intensity. It is well known, see Kahneman & Tversky (1979), that human behavior exaggerates for decisions under risk small probabilities, as described in prospect theory. This exaggeration applies also to the above extracted "natural" dynamics of volatility. One may assume that the people in the economy overreact to the observed ups and downs of aggregate wealth. When volatility should be high under the above derived normalized index dynamics in τ-time it becomes even higher in physical time and vice versa.

In Section 4 we will integrate the above revealed affine nature of aggregate wealth dynamics in an index model, which incorporates then also the typical overreactions in human behavior via a random market activity time. This time will be driven by the same nondiversifiable uncertainty that drives the index dynamics and will exaggerate the volatility to the extent observed in reality.

3 Stylized Empirical Facts

According to Popper (1934) one cannot "prove" the validity of a model. The best one can achieve is to find that one cannot falsify the candidate model but can falsify competing models based on empirical evidence. In this section we employ standard statistical and econometric techniques to establish for a well diversified equity index a list of stylized empirical facts. Deliberately, we rely on common and robust techniques and avoid any technicalities.

We use for our empirical analysis the total market equity index (with mnemonics TOTMKWD), downloaded from Datastream Thomson Reuters Financial in August 2012. This index is a market capitalization weighted world stock index, and very similar to the MSCI world index. In this paper, we call this equity index,

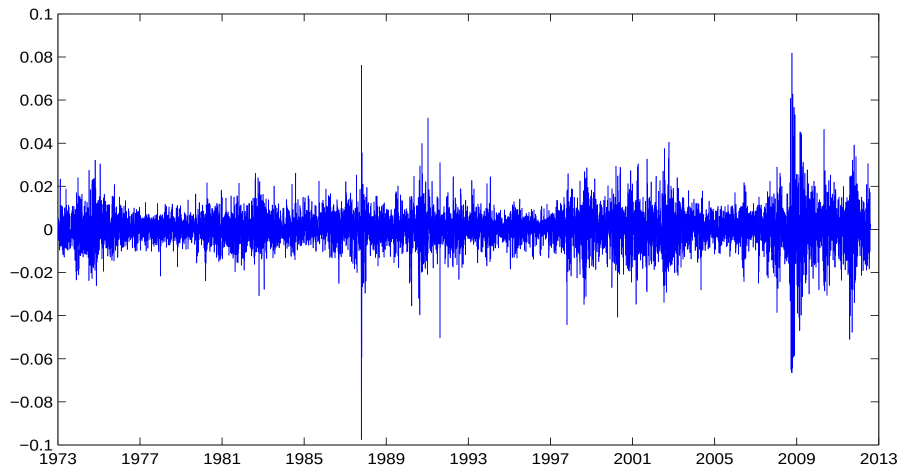

Figure 3.2: Log-returns of the MCI.

the market capitalization index (MCI). Fig. 3.1 displays the logarithm of the MCI while Fig. 3.2 shows the log-returns of the MCI.

The list of stylized empirical facts, established below, will allow us to circle in a parsimonious, tractable model that cannot be easily falsified with respect to these facts:

(i) Uncorrelated Returns

First, we studied the MCI denominated in the 26 currencies of the countries listed in Table 3.2. For each currency the autocorrelation of the log-returns was calculated for each shown number of days between observations and then averaged over the currencies, which provided in Fig. 3.3 the well-known typical graph; see e.g. Ghysels, Harvey & Renault (1996). It shows practically no correlation between the different returns. Here the horizontal axis gives the number of days between the observed returns. The autocorrelation function in Fig. 3.3 is, in principle, located between the displayed 95% upper and lower confidence bounds. In the literature this is a well accepted property of index returns. Therefore, we formulate our first stylized empirical fact:

Index log-returns are not correlated over time.

(ii) Correlated Absolute Returns

Similarly as above, also the autocorrelation for the absolute log-returns of the MCI has been estimated for each currency denomination. In Fig. 3.4 the resulting average of the estimated autocorrelation functions of the absolute log-returns for the 26 currency denominations of the MCI is displayed in dependence on the time lag in days. As known from many other studies,

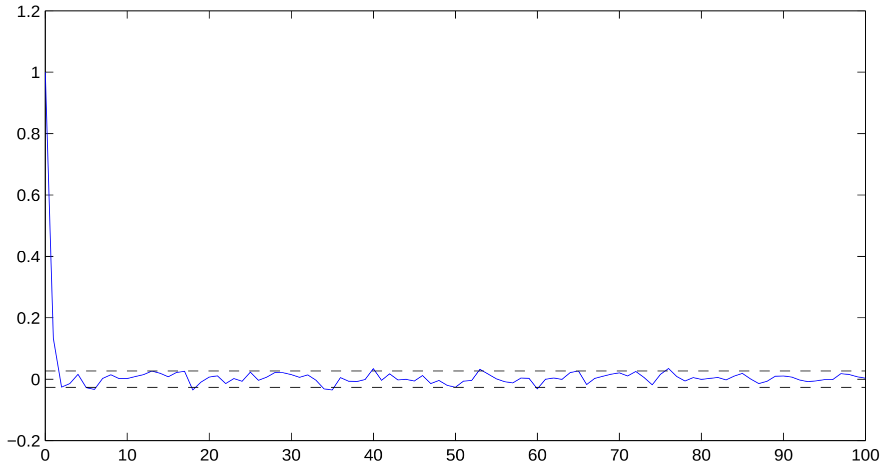

Figure 3.3: Average autocorrelation function for log-returns of the MCI in different currency denominations.

Table 3.1: Log-Maximum likelihood test statistic for daily, weekly and fortnightly log-returns of the MCI.

Frequency	Student-t	NIG	Hyperbolic	VG	ν
Daily	3.016652	1336.306309	4453.111995	5367.048317	3.495706
Weekly	0.000000	211.666854	519.162808	701.370317	4.307228
Fortnightly	3.338603	60.216977	204.104996	47.288206	4.216611

see e.g. Ghysels, Harvey & Renault (1996), one observes that this sample autocorrelation does not die away fast and remains after 100 days still far from the 95% confidence bound for the hypothesis that there may be no autocorrelation. Furthermore, the decay of the average autocorrelation does not seem to be exponential. Even for large lags of several months there is still some not negligible autocorrelation of absolute log-returns present. Note that the Black-Scholes model and many of its extensions, including exponential Lévy models, do not exhibit this property. Also this is in the literature a widely accepted empirical property of equity indices and we formulate the second stylized empirical fact:

The sample autocorrelation of absolute log-returns does not die away exponentially, and cannot be neglected for large lags.

(iii) Student-t Distributed Returns

From the 26 currency denominations with mostly 39 years of daily observations we have a substantial dataset of log-returns available, which provide

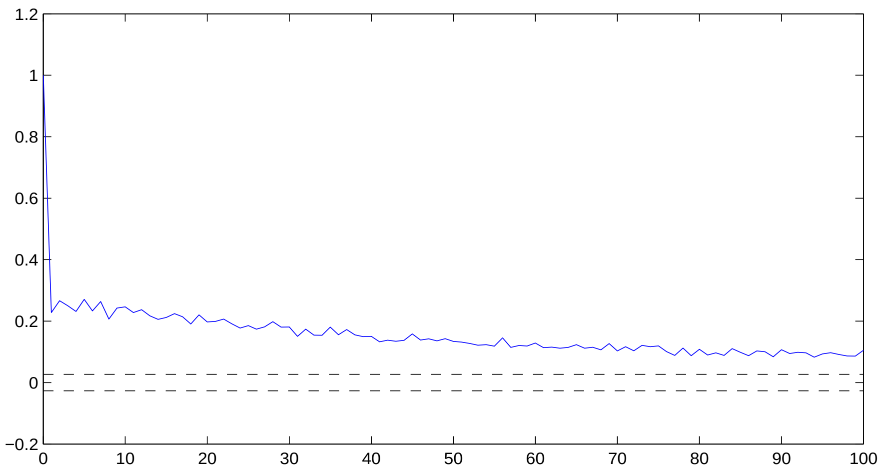

Figure 3.4: Average autocorrelation function for the absolute log-returns of the MCI in different currency denominations.

Table 3.2: Log-Maximum likelihood test statistic for different currency denominations of the MCI.

Country	Student-t	NIG	Hyperbolic	VG	ν
Australia	0.000000	58.129392	144.865134	180.029220	3.918181
Austria	1.000815	41.266882	157.562238	190.955439	3.435910
Belgium	0.976188	40.671955	154.030262	189.996360	3.458126
Canada	0.000000	42.354744	94.626898	124.885496	4.454300
Denmark	0.194751	35.909603	110.311722	144.178062	3.907690
Finland	3.953519	29.507246	156.290841	176.470426	3.192224
France	2.454694	33.126251	153.720450	186.278677	3.332276
Germany	1.089218	37.984695	146.623206	178.879859	3.462573
Greece	0.087889	47.616770	159.745413	185.004929	3.368001
Hong.Kong	0.955483	33.163802	142.601238	168.218205	3.293006
India	0.000000	58.935308	170.125958	208.765488	3.648135
Ireland	0.007503	66.903516	218.951365	254.213268	3.361688
Italy	3.975738	26.302040	144.201210	167.455552	3.244692
Japan	1.203367	42.032471	186.745356	218.934846	3.228296
Korea.S.	0.000000	100.310795	314.042722	345.682862	3.107851
Malaysia	0.040659	66.371816	210.194378	253.251366	3.438201
Netherlands	0.900068	40.155097	151.802950	185.510512	3.474006
Norway	0.089357	39.067234	112.438014	152.293627	4.001805
Portugal	2.253549	39.426104	188.698882	209.615521	3.150901
Singapore	0.315454	27.494392	99.564426	123.186925	3.592624
Spain	0.715989	47.820695	192.030088	219.961909	3.263888
Sweden	0.000000	68.297279	159.571420	200.409252	4.020877
Taiwan	0.723684	29.571185	120.256752	140.772751	3.358707
Thailand	0.972236	43.834495	225.116046	244.468484	2.924801
UK	0.949227	19.643975	68.567717	103.504763	4.253508
USA	0.138002	46.862320	155.995200	192.490293	3.566637

a total observation period of about 1000 years. Similarly as in Fergusson & Platen (2006) and Platen & Rendek (2008), for each of the 26 currency

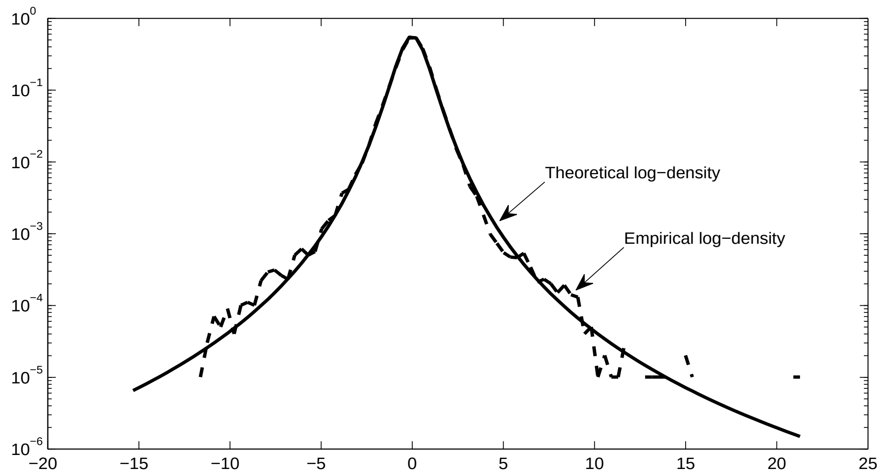

Figure 3.5: Logarithms of empirical density of normalized log-returns of the MCI and Student-t density with 3.5 degrees of freedom.

denominations we shifted the log-returns of the MCI so that their average for a given currency denomination becomes zero. For each currency denomination these shifted returns are then scaled such that a variance of one is estimated. Finally, all shifted and scaled returns are joined in one large dataset of $268,684$ daily normalized returns. Note, by choosing as object of study a global benchmark, the MCI, it became possible to form such a large dataset for log-returns where one can expect clear statistical results. The corresponding log-histogram for the entire sample of log-returns is shown in Fig. 3.5. This figure displays also the log-density of a Student-t distribution with 3.5 degrees of freedom. Remarkable is the excellent visual fit for the medium range of the log-return values and also for extreme log-returns. The latter are most important in risk management; see McNeil, Frey & Embrechts (2005). We notice also a slightly negative skew in the log-returns when compared to the shown symmetric Student-t log-density, which has been observed also in other studies; see e.g. Ghysels, Harvey & Renault (1996).

To obtain an idea about the significance of the above observed Student-t property, a standard maximum likelihood ratio test has been performed for the rich class of symmetric generalized hyperbolic (SGH) distributions, as described in detail in Platen & Rendek (2008); see also Barndorff-Nielsen (1977) and McNeil, Frey & Embrechts (2005). It turns out that the log-maximum likelihood test statistics for the weekly log-returns is with $0.00000012 < \chi^2_{0.001,1} \approx 0.000002$ such that one cannot reject with 99.9% significance the hypothesis that the Student-t distribution with 4.3 degrees of freedom is the underlying distribution, see Table 3.1. For daily and fortnightly log-returns the Student-t maximum likelihood test statistic is clearly the smallest when compared to the other special cases of the SGH distribution. A similar study was performed in Platen & Rendek (2008) with an equi-weighted world index, the EWI104s, which did not include the financial crisis 2007/2008. In that study for daily log-returns, the hypothesis that the Student-t distribution with 4.3 degrees of freedom is the underlying distribution could not be rejected at the 99.9% level of significance. The authors noticed in these kind of studies on diversified world stock indices that a few extreme log-returns, e.g. those of the recent financial crisis, can slightly distort the otherwise perfect Student-t fit. We conclude that it is difficult to identify with extreme significance the distribution and the exact parameters from the available data. However, the Student-t distribution as best fit for well diversified equity index log-returns appears to be a stylized fact.

We studied also separately daily log-returns of the MCI when denominated in each of the 26 different currencies with the results listed in Table 3.2. This table reports the log-maximum likelihood test statistics for different currency denominations of the MCI. In 5 out of the 26 currency denominations the hypothesis that the Student-t density is the true density, when nested in the class of SGH densities, cannot be rejected on a significance level of 99.9%. Models generating the following respective log-returns can be rejected for all currency denominations: the normal inverse Gaussian (NIG) density, appearing e.g. in asset price models of Barndorff-Nielsen (1997); the hyperbolic density, resulting from models e.g. in Eberlein & Keller (1995); and the variance gamma (VG) density, typical for models developed in Madan & Seneta (1990) and Carr et al. (2004). Additionally, in the last column of Table 3.2 we report the estimated degrees of freedom for the Student-t density, which range between 2.9 and 4.5. Here we emphasize again that a few extreme log-returns in a more than 30 year daily dataset can bring the estimate for the degrees of freedom easily down by half a degree.

Also other authors estimated the Student-t distribution from returns of equity indices; see e.g. Markowitz & Usmen (1996a, 1996b) and Hurst & Platen (1997). Recently, Alparslan, Tessitore & Usmen (2012) compared the best of the Pearson family of distributions with the best of the family of stable distributions. Their results strongly support the Student-t distribution for index log-returns when using a Bayesian approach.

We summarize the third stylized empirical fact:

Short and longer term log-returns appear, when estimated, as being Student-t distributed with about four degrees of freedom, exhibiting a slight negative skew.

(iv) Volatility Clustering

It is well-accepted that the volatility of an index is stochastic and clusters occasionally over time; see e.g. Ghysels, Harvey & Renault (1996) and

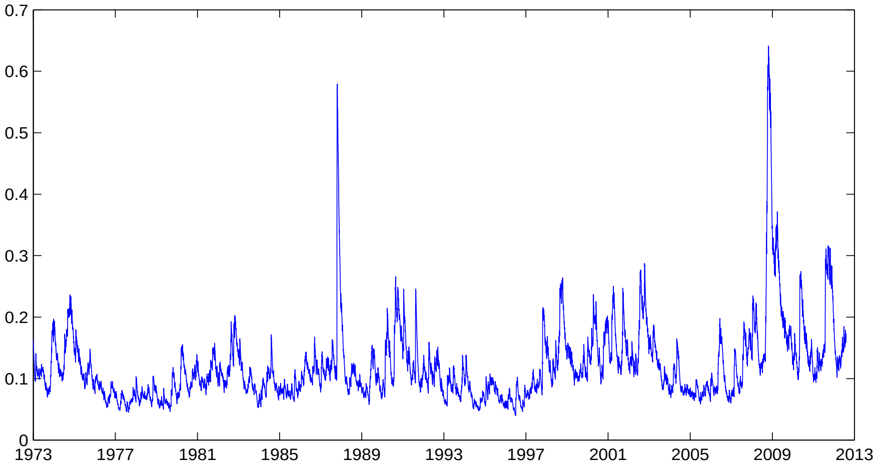

Figure 3.6: Estimated volatility from log-returns of the MCI.

the log-returns of the MCI displayed in Fig. 3.2. A standard estimation of volatility from the daily observed discounted MCI in US dollar denomination is shown in Fig. 3.6, where the squared volatility was estimated via a moving average with weight $\alpha\sqrt{\Delta} = 0.0569$ to each newly observed squared log-return, $\alpha = 0.92$, $\Delta = \frac{1}{261}$. This figure confirms for the MCI that its volatility is stochastic and shows clusters of higher values during some time periods. Furthermore, it is reasonable to conclude from the available observations of the MCI in different currency denominations that the volatility has approximately a stationary density. One has to acknowledge the fact that empirically one has so far only access to some moving average type estimate, as shown in Fig. 3.6. The hidden accurate theoretical volatility path of an index is almost impossible to observe. A volatility index, like the VIX, shown in Fig. 9.4 for the S&P500, gives a market perspective on some quantity closely related to the hidden volatility of the index.

The already mentioned wide range of literature on volatility modeling, including the ARCH and GARCH literature, which originated with Engle (1982), agrees on stochasticity, stationarity and clustering of volatility. The observable stationarity property is not reflected by CEV type models, see e.g. Cox (1975). Also models like the popular SABR model, see Hagan et al. (2002), which uses geometric Brownian motion to model volatility, are not consistent with volatility observations over long time periods. We formulate the fourth stylized empirical fact:

Volatility appears to be stochastic, exhibiting approximately stationary dynamics, with occasional clusters of higher volatility.

(v) Long Term Exponential Growth

For long term risk management, as required for pensions and insurance con-

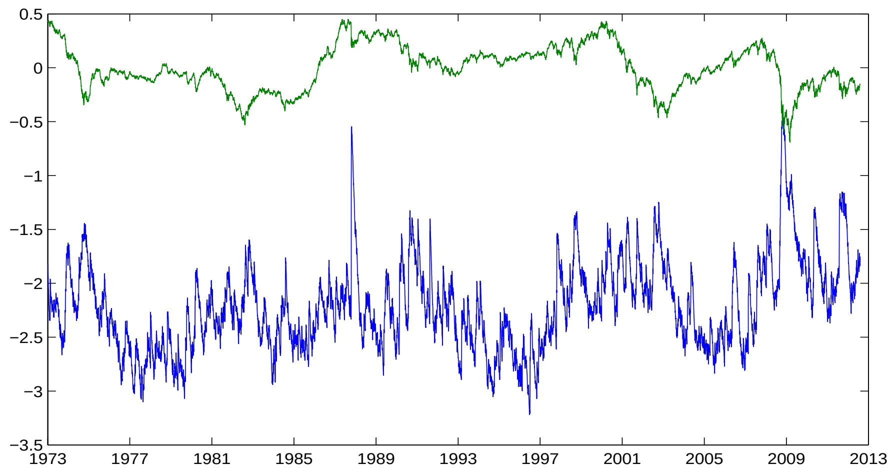

Figure 3.7: Logarithms of normalized discounted MCI (upper graph) and its volatility (lower graph).

tracts, the long term average growth of securities is important. In Fig. 7.1 the logarithm of the MCI, discounted by the US savings account, has been displayed. It seems to be reasonable to fit in Fig. 7.1 a trend line. Its slope measures the long term average growth rate of the discounted MCI. By removing this observed average growth from the logarithm of the discounted MCI one obtains the logarithm of the resulting normalized discounted MCI, which is displayed as upper graph in Fig. 3.7. It is reasonable to expect that the normalized discounted MCI could be modeled by a stochastic process that has approximately a stationary density. Many popular models are not consistent with the above mentioned stationarity property, e.g. generalizations of the Black-Scholes model, including popular stochastic volatility models like the Heston model, see Heston (1993). We summarize our observation in the fifth stylized empirical fact:

The discounted index exhibits in the long term on average exponential growth, and the accordingly normalized index appears to have approximately a stationary density.

(vi) Leverage Effect

It has been well documented since the work of Black (1976) and Rubinstein (1976) that the volatility of a normalized equity index appears visually to be negatively correlated with its volatility. Fig. 3.7 visualizes this property by plotting as upper graph the logarithm of the normalized discounted MCI and as lower graph the logarithm of the estimated volatility, previously shown in Fig. 3.6. Visually one notes that both processes appear to fluctuate mostly in opposite directions. Note that the logarithm of the volatility fluctuates in a much wider range. Despite the visual impression of strong

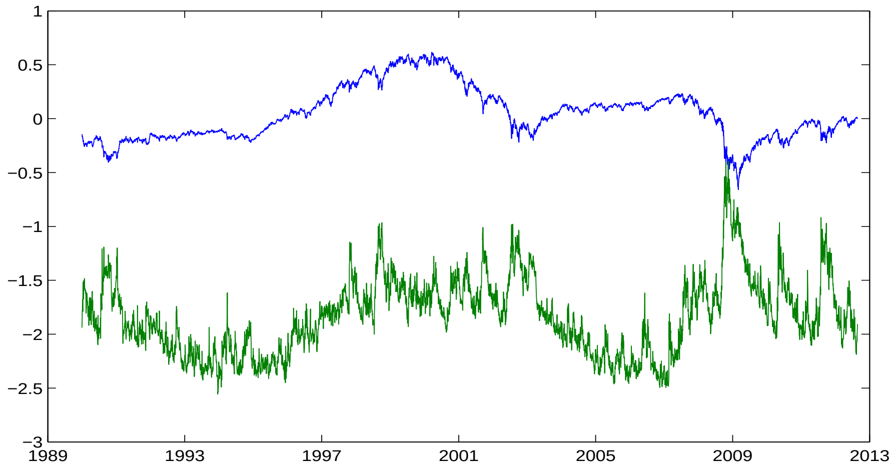

Figure 3.8: Logarithms of normalized discounted S&P500 (upper graph) and VIX (lower graph).

negative "dependence", the estimated correlation between the increments of both processes amounts only to -0.1. As has been made clear in recent work by Ait-Sahalia, Fan & Li (2012), and as will be confirmed later via simulation, the hidden theoretical volatility can be perfectly negatively correlated with the normalized index, but the estimated volatility may show only minor negative correlation with the normalized index. Given the strong visual negative "dependence" of the MCI and its volatility, this makes it difficult to identify any other source of uncertainty than the nondiversifiable uncertainty, which from an economic perspective may well drive both, the index fluctuations and the volatility fluctuations.

That there may be only one driving noise for the index and its volatility, is supported by the following fact: Strong negative correlation is detectable for equity indices and their volatility index, as long as the latter is available. Fig. 3.8 shows the logarithm of the normalized discounted S&P500 together with the logarithm of its volatility index, the VIX. The estimated correlation between their increments is -0.71. This shows that there is significant negative correlation between these two trajectories. Note that visually there is not much difference between Fig. 3.7 and Fig. 3.8. Simulations of an index with perfectly correlated volatility will later show that the estimated correlation is of similar magnitude as observed for the S&P500 and the VIX. We summarize the above observations in the sixth stylized empirical fact:

The dynamics of an index shows the leverage effect, where the volatility moves visually up when the normalized index moves down and vice versa. Both are potentially driven by the nondiversifiable uncertainty of the market.

(vii) Extreme Volatility at Major Market Downturns

In Fig. 3.7, similarly as in Fig. 9.4, one observes at major market downturns, e.g. in 1987 and 2007/2008, that the logarithm of volatility increases substantially more than the logarithm of the discounted index moves down. However, in periods of more moderate index movements, the magnitudes of volatility and index movements have been more in line. This means, in times of crises the increase of the volatility is much stronger than could be typically explained by, say, a simple function of the normalized index as model for volatility. On the other hand, there is a significant increase in trading activity observed in times of index decline, which contribute to increased volatility see e.g Ané & Geman (2000). This leads to the seventh and final stylized empirical fact in our list:

At major index downturns volatility increases significantly; more than a functional link between volatility and normalized index could explain. Moreover, market activity increases substantially during sharp index declines, which seems to contribute to increased volatility.

Any reasonably accurate model for the dynamics of the discounted MCI needs to reflect the above described stylized empirical facts. There may not exist too many parsimonious one- or two-component continuous diffusion models that could reflect to a sufficient degree all the above mentioned stylized empirical facts. For identifying the most suitable model class it would be extremely valuable to understand the nature of the index dynamics in a stylized manner. In Section 2 we conjectured a particular affine diffusion process, which theoretically should capture well the normalized aggregate wealth dynamics. We propose in the following a more general and still reasonably tractable class of parsimonious models that we will confront with the observed stylized empirical facts. The data should then tell us which specification of this model class seems to be most likely.

4 Index Model

This section considers an index model, which leans on the theoretically derived normalized aggregate wealth dynamics. It employs two Markovian components: a square root process for modeling the normalized index in some market activity time; and the inverse of a faster moving square root process for modeling the respective market activity. The normalized index and the market activity are driven by the same Brownian motion, which is modeling the nondiversifiable continuous market uncertainty.

Based on the above derived theoretical normalized aggregate wealth dynamics we propose a continuous time two-component model for the discounted index. Denote by S_t the discounted value of a (total return) index in calendar time

$t \geq 0$, denominated in units of the domestic savings account. This discounted index will be expressed by the product

$$S_t = A_{\tau_t} (Y_{\tau_t})^q \tag{4.1}$$

for $t \geq 0$. An exponential function A_{τ_t} of a given τ-time, the market activity time (to be specified below), models the long term average growth of the discounted index as

$$A_{\tau_t} = A \exp\{a \tau_t\} \tag{4.2}$$

for $t \geq 0$.

We use in (4.2) the initial parameter $A > 0$ and the long term average net growth rate $a \in \Re$ with respect to market activity time. One could interpret A_{τ_t} as the average value function, along which aggregate wealth of the economy evolves over time and to which the discounted index reverts back in the long run. We refer to Fig. 7.1, exhibiting the logarithm of the discounted MCI and its trendline, as some visual support for this assumption. It reflects part of the stylized empirical fact (v) on long term exponential growth.

Normalized Index

As a consequence of equation (4.1), the ratio $(Y_{\tau_t})^q = \frac{S_t}{A_{\tau_t}}$ denotes the normalized index at time t. This normalized index is assumed to form an ergodic diffusion process evolving according to τ_t-time. This means it represents a scalar diffusion process with stationary probability density. This property accommodates the remaining part of the stylized empirical fact (v), which requests a normalized index with stationary density. Fig. 7.2 shows the normalized MCI. It seems indeed realistic to model its dynamics by an ergodic process in the above described manner. Motivated by the arguments of Section 2, the dynamics of the normalized index are modeled by the qth power, $q > 0$, of a square root process $Y = \{Y_\tau, \tau \geq 0\}$ in τ-time; given by the SDE (4.3) below. We assume that the square root process has dimension $\delta > 2$ to keep it strictly positive. The square root process Y, as a component of the model, is highly tractable. We assume that it satisfies the SDE

$$dY_\tau = \left(\frac{\delta}{4} - \frac{1}{2} \left(\frac{\Gamma\left(\frac{\delta}{2} + q\right)}{\Gamma\left(\frac{\delta}{2}\right)} \right)^{\frac{1}{q}} Y_\tau \right) d\tau + \sqrt{Y_\tau}\, dW(\tau), \tag{4.3}$$

for $\tau \geq 0$ with $Y_0 > 0$. Only the two parameters $\delta > 2$ and $q > 0$ enter the SDE (4.3) together with its initial value $Y_0 > 0$. Note that the reference level for the square root process Y equals $\frac{\delta}{2} \left(\frac{\Gamma\left(\frac{\delta}{2}\right)}{\Gamma\left(\frac{\delta}{2}+q\right)} \right)^{\frac{1}{q}}$, which is then also its long run mean and one has asymptotically

$$\lim_{\tau \to \infty} \frac{1}{\tau} \int_0^\tau Y_s ds = \frac{\delta}{2} \left(\frac{\Gamma\left(\frac{\delta}{2}\right)}{\Gamma\left(\frac{\delta}{2} + q\right)} \right)^{\frac{1}{q}} \quad \text{P-a.s..} \tag{4.4}$$

Here $\Gamma(\cdot)$ denotes the gamma function and $W = \{W(\tau), \tau \geq 0\}$ denotes a Brownian motion in τ-time, which we specify further below.

Similarly, as discussed for the SDE (2.2), the choice of a positive power of the square root process Y in equation (4.1) creates a leverage effect in a simple and robust manner. This accommodates the stylized empirical fact (vi) on the leverage effect. The power of the square root process in the model has similarities to variants of the constant elasticity of variance (CEV) model, see Ross (1976). However, the volatility of the CEV model is not an ergodic process. The proposed model is a generalization of the minimal market model, see Chapter 13 in Platen & Heath (2010). It falls also into the wider category of local volatility function models, see Dupire (1993) and Derman & Kani (1994a).

The stationary density of the quantity $(Y_\tau)^q$ is explicitly given by the formula

$$p_{Y^q}(y) = \frac{\Gamma\left(\frac{\delta}{2}+q\right)^{\frac{\delta}{2q}}}{q\Gamma\left(\frac{\delta}{2}\right)^{\frac{\delta}{2q}+1}} y^{\frac{\delta}{2q}-1} \exp\left\{ -\left(\frac{\Gamma\left(\frac{\delta}{2}+q\right)}{\Gamma\left(\frac{\delta}{2}\right)} y\right)^{\frac{1}{q}} \right\} \tag{4.5}$$

for $y \geq 0$, see e.g. Platen & Heath (2010). The parametrization in (4.3) is chosen such that the long run mean for the process $(Y)^q$ equals one. More precisely, one obtains by the ergodic theorem

$$\lim_{\tau\to\infty} \frac{1}{\tau} \int_0^\tau (Y_s)^q ds = 1 \quad \text{P-a.s.} \tag{4.6}$$

The stationary density of the square root process Y is a gamma density with δ degrees of freedom and long run mean given in (4.4). This density generates for the normalized index and, thus, for the index, long term log-returns that when estimated appear to be Student-t distributed with δ degrees of freedom. This Student-t distribution results as a normal mixture distribution, where the inverse of the variance of the log-returns is proportional to Y_τ. The square root process has a stationary gamma density with δ degrees of freedom. In this manner, the qth power of the square root process in (4.1) accommodates the part of the empirical stylized fact (iii), which concerns the observed Student-t distribution for longer term returns. Due to the negative "dependence" between normalized index and its volatility in τ-time one models automatically the observed slight negative skewness of log-returns, expressed in the stylized empirical fact (iii).

The first component of the model, the qth power of the square root process Y describes how the normalized index reverts in τ-time back to its long term mean. This process models in τ-time the overall long term feedback mechanism of the normalized index, which brings in the long run the aggregate wealth back into the range of its long term average level. Furthermore, it ensures that the variance of increments of aggregate wealth is in τ-time proportional to total wealth.

Market Activity Time

Let us now focus on the second component of the model. According to the stylized empirical fact (iii), a Student-t distribution has to be obtained also when fitting short term index returns. Therefore, we introduce in this subsection market activity to reflect human behavior in economic activity and trading, which exaggerates the movements of volatility in reaction to moves of the normalized index.

The market activity process $M = \{M_t, t \geq 0\}$, reflects also the observation expressed in the stylized empirical fact (vii), where the market reacts to a major decrease in the level of the normalized index with significantly increased market activity. Trading activity is known to increase in relative terms when an index is falling and to decrease when it is rising, see e.g. Ané & Geman (2000). This results in speeding up or slowing down, respectively, the time scale under which the above discussed natural normalized index moves. To model conveniently the cumulative effect of speeding up and slowing down market activity, the above mentioned τ-time has been introduced, which is integrated market activity and called market activity time.

More precisely, we model the market activity time τ_t via the ordinary differential equation

$$d\tau_t = M_t dt \tag{4.7}$$

for $t \geq 0$ with $\tau_0 \geq 0$. Here we call the derivative of τ-time with respect to calendar time t the market activity $\frac{d\tau_t}{dt} = M_t$ at time $t \geq 0$. We will later see that M_t is, in reality, a fast moving process when compared to the square root process Y_{τ_t}. The stylized empirical fact (iii) requests that not only longer term log-returns but also short term returns of an index are estimated as being Student-t distributed. As we can see in Fig. 7.2, the overall long term feedback mechanism of Y_{τ_t} moves relatively slowly. Therefore, the market activity M_t needs to evolve such that it generates, via a mixture of normals, short term log-returns that when estimated indicate a Student-t distribution. Consequently, the market activity process M needs to have as stationary probability density an inverse gamma density.

Additionally, we argued earlier that potentially only the continuous nondiversifiable uncertainty should drive both the normalized index and the market activity. The squared volatility with respect to τ-time equals $\frac{1}{Y_\tau}$, where Y_τ is the square root process in (4.3). According to the stylized empirical fact (vii) the moves of the volatility in τ-time are in t-time exaggerated. Therefore, we model market activity, similarly to squared volatility, as the inverse of a square root process. More precisely, the process $\frac{1}{M} = \{\frac{1}{M_t}, t \geq 0\}$ is assumed to be a fast moving square root process in t-time with the dynamics

$$d\left(\frac{1}{M_t}\right) = \left(\frac{\nu}{4}\gamma - \epsilon\frac{1}{M_t}\right) dt + \sqrt{\frac{\gamma}{M_t}} dW_t, \tag{4.8}$$

for $t \geq 0$ with $M_0 > 0$, where $\gamma > 0$, $\nu > 2$ and $\epsilon > 0$. The Brownian motion $W = \{W_t, t \geq 0\}$ in t-time models the continuous nondiversifiable uncertainty of the market in t-time, and will be linked below in relation (4.11) to $W(\tau_t)$, which is the respective Brownian motion in τ-time. It is straightforward to confirm that the stationary density of the resulting market activity process M is an inverse gamma density with ν degrees of freedom. The resulting stationary density is given by the formula

$$p_M(y) = \frac{\left(\frac{2\epsilon}{\gamma}\right)^{\frac{1}{2}\nu}}{\Gamma\left(\frac{1}{2}\nu\right)} y^{-\frac{1}{2}\nu - 1} \exp\left\{ -\frac{2\epsilon}{\gamma}\frac{1}{y}\right\}, \tag{4.9}$$

for $y \geq 0$; see e.g. Section 12.4 in Platen & Heath (2010). As the result of normal mixing, this density generates short term index log-returns that when estimated, appear as being Student-t distributed with about ν degrees of freedom. One can show in the given parametrization that the long term average level for the inverse of market activity equals $\frac{\nu}{4}\frac{\gamma}{\epsilon}$, that is,

$$\lim_{t\to\infty} \frac{1}{t} \int_0^t \frac{1}{M_s} ds = \frac{\nu}{4}\frac{\gamma}{\epsilon} \quad \text{P-a.s.} \tag{4.10}$$

The Brownian motion $W(\tau)$, which models in market activity time the long term nondiversifiable uncertainty driving Y_τ, is linked to the standard Brownian motion $W = \{W_t, t \geq 0\}$ in t-time in the following manner:

$$dW(\tau_t) = \sqrt{\frac{d\tau_t}{dt}} dW_t = \sqrt{M_t} dW_t \tag{4.11}$$

for $t \geq 0$ with $W_0 = 0$.

The proposed index model is a Markovian two-component model, driven only by one Wiener process $W = \{W_t, t \geq 0\}$. The two components are Y_{τ_t} and $\frac{1}{M_t}$ that solve the SDEs (4.3) and (4.8), respectively. When substituting in the SDE (4.3) formally τ by τ_t, to characterize together with the SDE (4.8) the dynamics of the two-dimensional state variable $(Y_{\tau_t}, \frac{1}{M_t})$, the model is only driven by the Brownian motion $W = \{W_t, t \geq 0\}$. The full specification of the dynamics of the model is, therefore, given by the two SDEs (4.3) and (4.8) together with the respective initial conditions, where $W = \{W_t, t \geq 0\}$ models nondiversifiable uncertainty in t-time.

5 Modeled Volatility and Market Activity

We can now study and apply the proposed model in many ways. This section briefly discusses some of its properties concerning volatility and market activity. First, let us study the resulting expected rate of return and volatility of the discounted index.

Expected Rate of Return

By application of the Itô formula one obtains from (4.1), (4.2), (4.3), (4.7) and (4.8) for the discounted index S_t the SDE

$$dS_t = S_t \left(\mu_t dt + \sigma_t dW_t\right) \tag{5.1}$$

for $t \geq 0$, with initial value $S_0 = A_0 (Y_0)^q$ and expected rate of return

$$\mu_t = \left(\frac{a}{M_t} - \frac{q}{2} \left(\frac{\Gamma\left(\frac{\delta}{2} + q\right)}{\Gamma\left(\frac{\delta}{2}\right)} \right)^{\frac{1}{q}} + \left(\frac{\delta}{4} q + \frac{1}{2} q(q-1) \right) \frac{1}{M_t Y_{\tau_t}} \right) M_t. \tag{5.2}$$

Obviously, short term index log-returns are approximately uncorrelated, as requested by the stylized fact (i); see also Fig. 11.2.

Volatility

The volatility with respect to t-time emerges in the form

$$\sigma_t = q \sqrt{\frac{M_t}{Y_{\tau_t}}}. \tag{5.3}$$

Obviously, it is a function of the two square root processes Y_{τ_t} and $\frac{1}{M_t}$.

Autocorrelation

Due to the volatility (5.3), the absolute returns of S near time t are on average approximately proportional to $\sqrt{\frac{M_t}{Y_{\tau_t}}}$. Consequently, since Y is slow moving the correlation for two absolute log-returns near time t and $t+T$, respectively, is for small T determined by the correlation between $\sqrt{M_t}$ and $\sqrt{M_T}$, which can be shown to decline exponentially fast since M is a fast moving scalar diffusion process; see (4.8). On the other hand, when the time lag T is relatively large, then the correlation between the respective absolute returns is approximately that between $\frac{1}{\sqrt{Y_{\tau_t}}}$ and $\frac{1}{\sqrt{Y_{\tau_t+T}}}$. As we have discussed earlier, $\frac{1}{\sqrt{Y_{\tau_t}}}$ is moving rather slowly and the resulting correlation remains substantial even after several months. Similar to Fig. 3.4 the Fig. 11.3 shows the average autocorrelation of absolute returns under the proposed model obtained from simulated data, which confirms the above remarks. This reflects the stylized empirical fact (ii), where the correlation of absolute log-returns does not die out fast and is also not exponentially declining.

Obviously, the volatility is stochastic and generates under the model clusters of outbursts of volatility, as will be also confirmed when simulating paths of the index and its corresponding volatility in Section 10; see e.g. Fig. 10.4. This property accommodates the stylized empirical fact (iv).

3/2 Volatility Model

Of particular interest for the long term dynamics of squared volatility under the proposed model is by relation (5.3) the inverse $\frac{1}{Y_\tau}$ of the square root process with respect to τ-time. By (4.3) one obtains via the Itô formula the SDE

$$d\left(\frac{1}{Y_\tau}\right) = \left(\frac{1}{2}\left(\frac{\Gamma\left(\frac{\delta}{2}+q\right)}{\Gamma\left(\frac{\delta}{2}\right)}\right)^{\frac{1}{q}}\frac{1}{Y_\tau} + \left(1-\frac{\delta}{4}\right)\left(\frac{1}{Y_\tau}\right)^2\right)d\tau - \left(\frac{1}{Y_\tau}\right)^{\frac{3}{2}}dW(\tau) \tag{5.4}$$

for $\tau \geq 0$. This means that the factor $\frac{1}{Y_\tau}$ in the formula for squared volatility

$$\sigma_t^2 = \frac{q^2 M_t}{Y_{\tau_t}}, \tag{5.5}$$

see (5.3), follows in τ-time a $\frac{3}{2}$-volatility model, which was suggested e.g. in Platen (1997). Some versions of $\frac{3}{2}$-volatility models appeared, for instance, in Lewis (2000) and more recently in Carr & Sun (2007). Interestingly, the latter authors provided arguments from the perspective of volatility derivative pricing and hedging which support the choice of a $\frac{3}{2}$-volatility model for a diversified index. We will see in Section 9 that our model is in line with empirical evidence on volatility derivatives. Note that the long term average level for $\frac{1}{Y_\tau}$ can be calculated and equals $\frac{2}{\delta-2}\left(\frac{\Gamma\left(\frac{\delta}{2}+q\right)}{\Gamma\left(\frac{\delta}{2}\right)}\right)^{\frac{1}{q}}$. One obtains by the ergodic theorem

$$\lim_{\tau\to\infty}\frac{1}{\tau}\int_0^\tau \frac{1}{Y_s}ds = \frac{2}{\delta-2}\left(\frac{\Gamma\left(\frac{\delta}{2}+q\right)}{\Gamma\left(\frac{\delta}{2}\right)}\right)^{\frac{1}{q}} \quad \text{P-a.s..} \tag{5.6}$$

Finally, we recall that due to the perfect negative "dependence" between the normalized index and its volatility the log-returns of the index exhibit under the model a slight negative skew, which has been mentioned under the stylized empirical fact (iii).

Market Activity

By the fact that M_t has an inverse gamma density with ν degrees of freedom and negative first moment $\frac{\nu}{4}\frac{\gamma}{\epsilon}$, the mean of M_t is explicitly known. By the ergodic theorem this mean amounts to

$$\lim_{t\to\infty}\frac{1}{t}\int_0^t M_s ds = \frac{4}{\nu-2}\frac{\epsilon}{\gamma} \quad \text{P-a.s.} \tag{5.7}$$

Hence, for the proposed model one obtains the asymptotic relation

$$\lim_{h\to\infty}\frac{\tau_{t+h}-\tau_t}{h} = \frac{4}{\nu-2}\frac{\epsilon}{\gamma} \quad \text{P-a.s.} \tag{5.8}$$

for $t \geq 0$. Thus, increments of market activity time can be approximated asymptotically over long time periods h in t-time by the formula

$$\tau_{t+h} - \tau_h \approx \frac{4}{\nu - 2} \frac{\epsilon}{\gamma} h \tag{5.9}$$

for h sufficiently large, $h \in (0, \infty)$. Therefore, when quantifying long-term effects, as is the case for many long dated derivatives, it may turn out to be sufficient to employ only average τ-time by using the approximation

$$\tau_t \approx \tau_0 + \frac{4}{\nu - 2} \frac{\epsilon}{\gamma} t, \tag{5.10}$$

$t \geq 0$. This is a convenient property of the model. Essentially, in the long run we have only to deal with a one component model, characterized by the square root process Y, which is highly tractable and runs then in average τ-time for long dated contracts. For short term index derivatives the market activity is relevant and cannot be neglected.

Due to the volatility formula (5.3) and the SDEs (4.3) and (4.8) the fluctuations of both processes $\frac{1}{Y_{\tau_t}}$ and M_t are similarly driven by the fluctuations of the same Brownian motion, $W = \{W_t, t \geq 0\}$. Consequently, one obtains a much stronger reaction of the volatility process to extreme moves of the nondiversifiable uncertainty W than would be typical for standard scalar diffusion models or subordinated stochastic volatility models with independent subordinator. The product of two scalar diffusions in the formula (5.3) for the volatility makes the proposed model very realistic, as will be confirmed in Section 7. It encapsulates the fact that there is a close relationship between the random moves of the normalized index value Y_{τ_t}, that is, the index itself and those of the market activity M_t, which is largely driven by the behavior of market participants.

The proposed model can easily be made more flexible via extensions, e.g. allowing parameters to be time dependent, including a more flexible local volatility function, introducing a second Brownian motion or adding jumps. However, in Section 7 we will be able to demonstrate when fitting the model that we can reduce the number of flexible parameters and extract a parsimonious stylized model, which represents the affine aggregate wealth dynamics conjectured in Section 2.

6 Modeling under the Benchmark Approach

Now, we are going to discuss the proposed model in a financial modeling framework that goes considerably beyond the currently widely used classical no-arbitrage framework.

Benchmark Approach

The benchmark approach, see Platen (2011) and Platen & Heath (2010), is a general financial market modeling framework that goes beyond the classical no-arbitrage paradigm; see Ross (1976), Harrison & Kreps (1979) and Delbaen & Schachermayer (1994). The approach uses the numéraire portfolio (NP), see Long (1990), as central building block. It has been shown in Platen & Heath (2010) and Platen & Rendek (2012) that a diversified equity index, like the MCI, is a good proxy of the NP. Consequently, under the proposed model the SDE (5.1) could be interpreted as the SDE describing the evolution of the discounted NP of the given investment universe.

Due to the SDE (5.1) and the Itô formula, the dynamics for the benchmarked savings account $\hat{B}_t = \frac{1}{S_t}$, which is the inverse of the discounted NP, is characterized by the SDE

$$d\hat{B}_t = \hat{B}_t \left(\left(-\mu_t + \sigma_t^2 \right) dt - \sigma_t dW_t \right), \tag{6.1}$$

for $t \geq 0$, see (5.2) and (5.3). It follows for

$$\sigma_t^2 \leq \mu_t \tag{6.2}$$

for all $t \geq 0$ that the benchmarked savings account $\hat{B}_t$ forms an $(\underline{\mathcal{A}}, P)$-supermartingale. This is a stochastic process where its current value is greater or equal than its expected future values. This supermartingale property is the key property of any benchmarked nonnegative security under the benchmark approach, see Platen (2011). Since a nonnegative supermartingale that reaches zero will always remain at zero, this property eliminates any possibility for, so called, *strong arbitrage* in the sense of Platen (2011), which is equivalent to the notion of arbitrage in Loewenstein & Willard (2000).

Assumptions on the Model

To guarantee almost surely in the proposed model the absence of strong arbitrage, that is the inequality (6.2), one has by (5.2) and (5.3) to satisfy the following two conditions:

Assumption 6.1 *First, the dimension δ of the square root process Y needs to satisfy the equality*

$$\delta = 2(q+1). \tag{6.3}$$

Assumption 6.2 *The long term average net growth rate a with respect to τ-time has to satisfy the inequality*

$$\frac{q}{2} \left(\frac{\Gamma\left(2q+1\right)}{\Gamma\left(q+1\right)} \right)^{\frac{1}{q}} \leq a. \tag{6.4}$$

Assumption 6.1 is necessary for the supermartingale property of the benchmarked savings account. Assumption 6.2 guaranties then that the long term average net growth rate, denoted by a, is high enough to make the benchmarked savings account a supermartingale. These two assumptions guarantee jointly that the savings account, when denominated in units of the NP, becomes an $(\underline{\mathcal{A}}, P)$-supermartingale under the proposed model. This means, $\hat{B}_t$ is then satisfying the SDE

$$d\hat{B}_t = \hat{B}_t \left(\left(\frac{q}{2} \left(\frac{\Gamma\left(2q+1\right)}{\Gamma\left(q+1\right)} \right)^{\frac{1}{q}} - a \right) M_t dt - q \sqrt{\frac{M_t}{Y_{\tau_t}}} dW_t \right) \tag{6.5}$$

with zero or negative drift for all $t > 0$. The latter property makes $\hat{B}$ an $(\underline{\mathcal{A}}, P)$-supermartingale.

Beyond Classical No-arbitrage

If equality holds in relation (6.4), then the SDE (6.5) is driftless. Note however, that this does not mean that $\hat{B}$ forms then a true martingale. It is in this case a nonnegative strict local martingale and, thus, a strict supermartingale and not a martingale.

In a complete market the benchmarked savings account, normalized to one at the beginning, represents the Radom-Nikodym derivative for the risk neutral measure. Under the classical paradigm the benchmarked savings account would have to be a true martingale; see Delbaen & Schachermayer (1994). It is important to emphasize that we identified here a model that goes beyond classical no-arbitrage settings. It goes even beyond the benchmark approach as formulated in Platen & Heath (2010), where the benchmarked savings account is assumed to be a local martingale. For the proposed model this may be only the case when equality holds in (6.2). However, the proposed model is well covered by an extension of the benchmark approach formulated in Platen (2011). The SDE for the benchmarked savings account does not need to be driftless. It can have a negative drift. We will see in Section 7 the fit of the model to historical data, where a clear negative drift is evident for the analyzed index. This leads the model far away from the classical no-arbitrage paradigm, and allows it to explain "puzzles" and "anomalies" that have been pointed out in the literature when applying the classical no-arbitrage approach. The following indicates such a "puzzle".

Risk Premium Puzzle

By applying the Assumptions 6.1 and 6.2 to the proposed model, one obtains by (5.2) the risk premium

$$\mu_t = \sigma_t^2 + M_t \left(a - \frac{q}{2} \left(\frac{\Gamma(2q+1)}{\Gamma(q+1)} \right)^{\frac{1}{q}} \right) \geq \sigma_t^2 \tag{6.6}$$

for all $t \geq 0$. Obviously, since the discounted index is the NP in our complete market μ_t can be here higher than the classical risk premium σ_t^2 of the NP, which is the square of the volatility of the NP. Under the benchmark approach described in Platen (2011), a higher risk premium is permitted. We emphasize that, the risk premium puzzle, see Mehra & Prescott (1985), is in our generalized benchmark framework not a "puzzle". It simply states the fact that the expected return of the NP is in reality larger than the square or its volatility. There is no economic reason to stop the expected return to reach a certain level. The classical no-arbitrage paradigm is making restrictive assumptions that do not coincide with reality. For empirical reasons we will have to go in our modeling beyond classical no-arbitrage assumptions to capture realistically the observed long term dynamics of the aggregate wealth.

Pricing of Derivatives

Under the benchmark approach one uses the NP as numéraire or benchmark. The pricing of derivatives applies the real world pricing formula, see Platen (2011), which yields the benchmarked derivative price as real world conditional expectation of the corresponding benchmarked payoff. To calculate such a price for a contingent claim that involves the discounted NP, one can employ the proposed model. The transition density of the square root process in τ-time is a non-central chi-square density with $\delta = 2(q+1)$ degrees of freedom, which makes this component of the model very tractable. For many long dated contingent claims the τ-time can be expected to be well approximated via average τ-time, according to (5.9).

For the pricing of short dated derivatives under the proposed model, numerical techniques can be employed, e.g. similar to those described in Section 13.4 in Platen & Heath (2010). The proposed model can be expected to recover well the typically negatively skewed implied volatility surface of index options. The random fluctuations of market activity will turn out to be crucial for realistic modeling of short dated index derivatives. They generate the observed strong curvature of the implied volatility surface of index options near the strike and close to maturity.

The proposed model uses only one Brownian motion to drive the two diffusion processes. The three initial and five structural parameters are: the parameter $A \geq 0$ in (4.2) for fitting the initial value of the average exponential growth part; the initial value $M_0 > 0$ of the market activity; the initial value $Y_0 > 0$ of the square root process; the long term average net growth rate $a > 0$ (with respect to τ-time) of the discounted index; the power $q > 0$ of the square root process when forming the normalized index; the parameter q determines also the dimension $\delta = 2(q+1) > 2$, see (6.3), of the square root process; the degrees of freedom $\nu > 2$, see (4.8), of the stationary gamma density of the inverse of the market activity; the reference level parameter ϵ for the market activity, see (4.8) and (5.9); and the scaling parameter $\gamma > 0$ in the diffusion coefficient of the SDE (4.8) for the inverse of market activity. All eight parameters have a clear meaning and can be directly estimated from time discrete observations of the index, as will be demonstrated in the next section. Moreover, we will demonstrate in the next section that by reasoning, as presented in Section 2, and by empirical evidence one can reduce the number of structural parameters to three.

7 Fitting the Model

It is paramount that the proposed model can be easily fitted in a robust manner to historical index data. This section illustrates a simple and robust step by step method for fitting the proposed model to historical index data. It will turn out that we can fix some of the parameters, which will yield a stylized version of the model. Below we separate the estimation of the parameters into the following steps:

Step 1: Normalization of Index

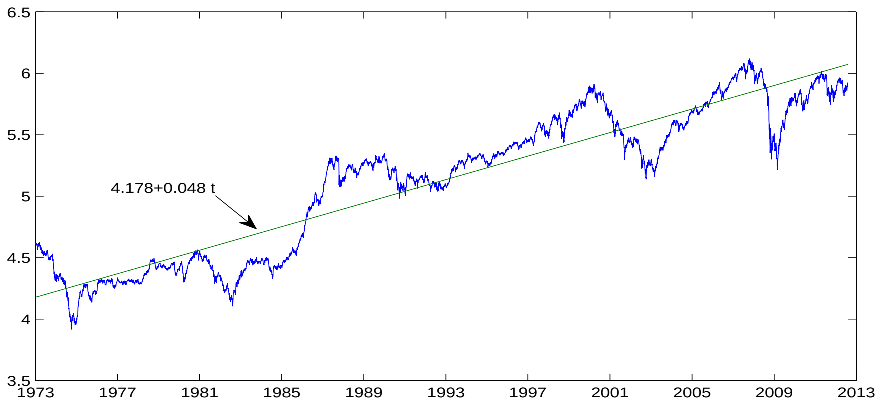

Figure 7.1: Logarithm of the discounted MCI and linear fit.

A linearly regressed function of calendar t-time to the path of the logarithm of the daily observations of the discounted MCI, as shown in Fig. 7.1, yields the straight line $4.178 + 0.048t$. The normalized MCI is then obtained by dividing the discounted index by the long term approximation for the exponential function A_{τ_t}, given on the right hand side of relation (7.1), obtained from (4.2) using (5.9). This means, we set

$$A_{\tau_t} \approx A \exp\left\{\frac{4a\epsilon}{\gamma(\nu-2)}t\right\}, \tag{7.1}$$

for $t \geq 0$, and read off from the above mentioned linear regression the estimate $\frac{4a\epsilon}{\gamma(\nu-2)} \approx 0.048$. The resulting discounted MCI $(Y_{\tau_t})^q$ is plotted in Fig. 7.2 with respect to physical t-time, where the initial parameter $A = 65.21$ is estimated by making the average of $(Y\tau_t)^q$ approximately to one, as required by (4.6).

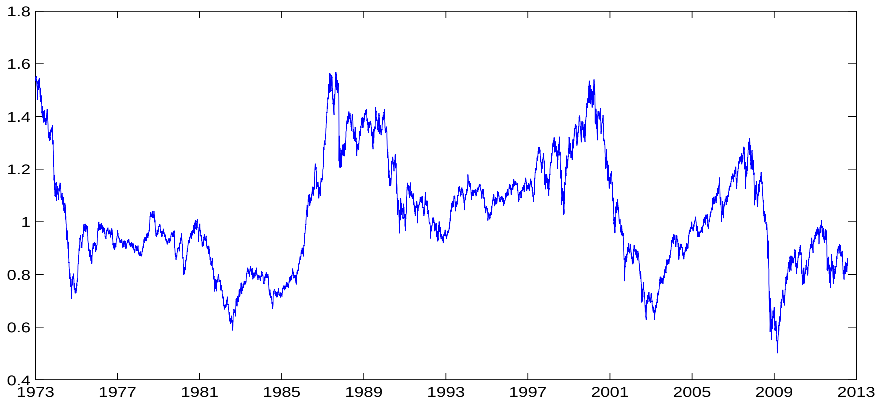

Figure 7.2: Normalized MCI.

Step 2: Power q

We recall our results for the normalized and scaled log-returns for the 26 currency denominations of the MCI, the logarithm of their histogram was displayed in Fig. 3.5. Maximum-likelihood Student-t fits are provided in Table 3.1 for daily, weekly and fortnightly log-returns. They estimate about four degrees of freedom. We emphasized that one needs a very large time window to estimate with high significance the degrees of freedom. One can see later in Section 11 in Fig. 11.4 and Table 11.3, using simulated data under the proposed model with $\delta = 4$ that for 40 years of daily observations it is only possible to estimate the degrees of freedom of log-returns with an error where the estimate could easily yield one degree more or less than four. For instance, the less than 40 years of daily data for the US denomination of the MCI are still not sufficient for the task of estimating the degrees of freedom more precisely than expecting it to be between 3 and 5. Fortunately, it will turn out in our step by step estimation procedure that there is not much influence of the choice by the degrees of freedom $\delta = 2(q+1)$ on the estimated values of the other parameters when fitting the model. Consequently, when following the economic arguments in Section 2, which conjectured asymptotically a time transformed square root process for the dynamics of the normalized index, there is a reason for setting $q = 1$, which provides the square root in the diffusion coefficient of the normalized index. Therefore, according to the theoretically derived aggregate wealth dynamics we specify the proposed model by fixing the power q to one. Thus, the dimension of the square root process amounts to $\delta = 4$ because of (6.3).

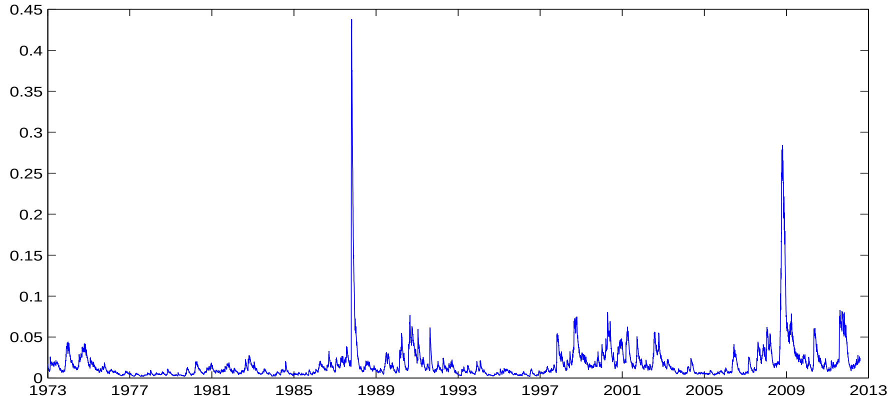

Figure 7.3: Estimated trajectory of the market activity M_t.

Step 3: Observing Market Activity

In Ané & Geman (2000) it has been shown that when subordinating intraday log-returns on observed trading activity, one obtains Gaussian distributed conditional returns. This is what our proposed model would predict for intraday log-returns. Intraday data were not available to us for sufficiently long time periods that we could use to fit our model. Instead we construct an observable proxy for market activity in the following way: By (4.3), (4.7) and an application of the Itô formula, one obtains as time derivative of the quadratic variation for $\sqrt{Y_{\tau_t}}$ the expression

$$\frac{d[\sqrt{Y}]_{\tau_t}}{dt} = \frac{1}{4}\frac{d\tau_t}{dt} = \frac{M_t}{4}, \tag{7.2}$$

which is proportional to market activity. The observed market activity time $\tau_t = \int_0^t M_s ds$ is shown in Fig. 8.1. It is a well observable process which tells us with its slope when market activity is high or low. In order to obtain an estimated proxy for the trajectory of the market activity process $M = \{M_t, t \geq 0\}$, appearing in (7.2), we perform some exponential smoothing of the empirical derivative of the quadratic variation $[\sqrt{Y}]_t$. Of course, other smoothing methods could potentially be used. However, we realized that most smoothing methods yielded very similar outcomes. We found the standard exponential smoothing method to be sufficient and rather robust with respect to the choice of the weight parameter $\alpha > 0$, which will be specified below.

The estimation of the trajectory of the market activity process M is performed using daily observations. First, the "raw" time derivative $Q_t = \frac{d[\sqrt{Y}]_{\tau_t}}{dt}$ at the ith observation time $t = t_i$ is estimated from the finite difference

$$\hat{Q}_{t_i} = \frac{[\sqrt{Y}]_{\tau_{t_{i+1}}} - [\sqrt{Y}]_{\tau_{t_i}}}{t_{i+1} - t_i} \tag{7.3}$$

for $i \in \{0, 1, \dots\}$. Second, exponential smoothing is applied to the observed finite differences according to the recursive standard moving average formula

$$\tilde{Q}_{t_{i+1}} = \alpha\sqrt{t_{i+1} - t_i}\hat{Q}_{t_i} + (1 - \alpha\sqrt{t_{i+1} - t_i})\tilde{Q}_{t_i}, \tag{7.4}$$

$i \in \{0, 1, \dots\}$, with weight parameter $\alpha > 0$. It is clear that the above smoothing depends on the observation frequency and the weight parameter with which new values enter the moving average calculation. We found that a smoothing parameter of about $\alpha \approx 0.92$ delivered a robust estimate for the trajectory of the market activity process. This parameter and its neighboring values provided for daily but also for the two-day observation frequency a very similar trajectory that we use here as proxy for the discretely observed market activity process M. Fig. 7.3 displays the resulting trajectory of M_t for daily observations, when interpreting this value as estimate of $4\frac{d}{dt}[\sqrt{Y}]_{\tau_t}$, for $t \geq 0$. Here an initial value of $M_0 \approx 0.0175$ emerged and the time average of the trajectory of $(M_t)^{-1}$ amounted to 113.92.

The estimated trajectory of the market activity process, shown in Fig. 7.3, appears to be that of a rather "fast" moving process when compared with the trajectory of the square root process Y, representing the normalized MCI shown in Fig. 7.2. This means, we are dealing in our model with two different time scales. These are the t-time and the τ-time. The "slow" moving square root process Y moves in τ-time and is modeled according to the affine nature of aggregate wealth dynamics. The "fast" moving market activity process M evolves in t-time and models the reactions of market participants to changes in the level of the normalized index, generating some exaggerations in volatility. Changes in market activity are triggered by observed random ups and downs of the normalized index. One can see this when comparing Fig. 7.2 and Fig. 7.3. Market activity, when compared to the squared volatility $\frac{1}{Y_{\tau_t}}$ in τ-time, appears to move mostly together up and down. Therefore, it appears sufficient that we assumed that, all fluctuations in the model are driven by the nondiversifiable uncertainty of the market. It seems to be difficult to find evidence that the driving uncertainty for the normalized index and the market activity have to be different.

Step 4: Parameter γ

Now, we would like to identify the parameter γ in the diffusion coefficient in the SDE (4.8) for the inverse $\frac{1}{M_t}$ of the market activity process. Fig. 7.4 plots the quadratic variation of the square root of the estimated process $\frac{1}{M}$. Given that $\frac{1}{M}$ is assumed to be a square root process, this quadratic variation should be ideally a straight line. In a first approximation the graph in Fig. 7.4 confirms this. However, as can be seen from (7.4) and will be shown in Section 10 with simulated data, such discretely formed proxy for the quadratic variation, derived from to the estimated proxy of $\frac{1}{M}$, is not a perfect straight line, see Fig. 10.8. The deviations result from the procedure of exponential smoothing when estimating the proxy for the market activity process M. We assume now that a straight line

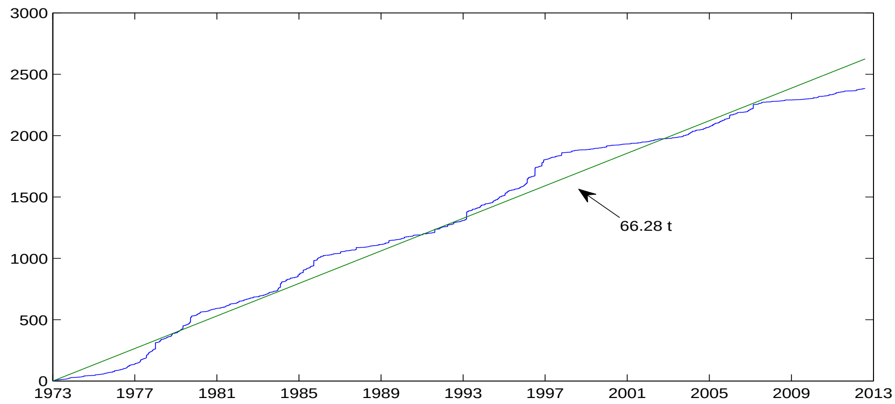

Figure 7.4: Quadratic variation of the square root of the estimated trajectory of $\frac{1}{M}$ with linear fit.

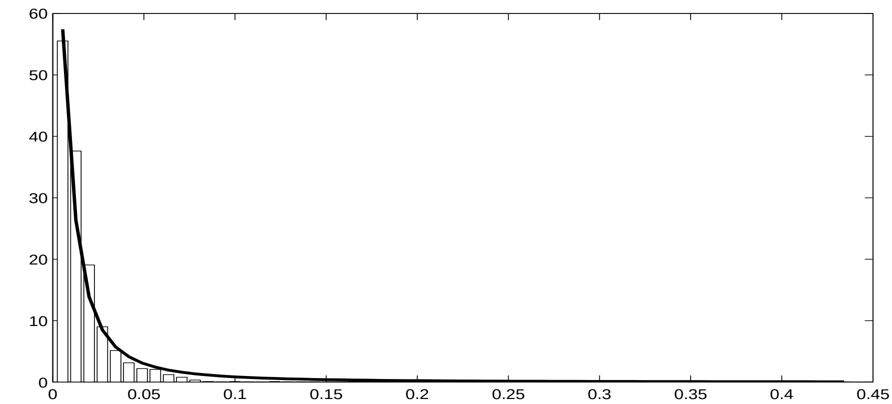

Figure 7.5: Histogram of market activity M with inverse gamma fit.

can be fitted (by linear regression) to such observed quadratic variation and the parameter γ can be estimated from the slope of this line. Our estimate for the slope equals here 66.28. Since under the proposed model we have $\frac{d}{dt}\left[\sqrt{\frac{1}{M}}\right]_t = \frac{1}{4}\gamma$, we obtain $\gamma \approx 265.12$.

Step 5: Parameters ν and ϵ

Fig. 7.5 plots the histogram for the trajectory of the proxy of the market activity M using daily observations. This fit appears to be realistic. The maximum likelihood estimation of the stationary inverse gamma density of the market activity process yields $\nu \approx 3.75$ degrees of freedom and mean $\frac{4\epsilon}{\gamma(\nu-2)} \approx 0.0175$; see (5.7). Since $\gamma \approx 265.12$ this yields $\epsilon \approx 2.18$.

The stylized fact (iii) requests for long term and short term log-returns of the discounted index a Student-t distribution with about the same degrees of freedom. Therefore, we simplify the model further. For the stylized version of the model we assume that it generates short term log-returns with the same degrees of freedom as long term log-returns. This means, we have set in the stylized version of the proposed model $\nu = \delta = 4$. This reduces the number of parameters to six that have to be estimated for the stylized version of the model.

Step 6: Long Term Average Net Growth Rate

Since we have now estimated the parameters γ, ν and ϵ, and know that $\frac{d\tau_t}{dt} \approx \frac{4\epsilon}{\gamma(\nu-2)} \approx 0.0175$, it follows from (7.2) and the slope $0.048 \approx a\frac{4\epsilon}{\gamma(\nu-2)}$ of the trend line in Fig. 7.1 that for the long term average net growth rate we have an estimate of about $a \approx 2.55$. This estimated value of a satisfies clearly the inequality (6.4), where its left hand side equals $\frac{1}{2}\frac{\Gamma(3)}{\Gamma(2)} = 1$. Most importantly we observe that when the MCI is interpreted as the numéraire portfolio (NP) under the benchmark approach, the benchmarked savings account is by (6.4) an $(\underline{\mathcal{A}}, P)$-supermartingale with negative drift under the proposed model. It seems to be far from being a local martingale, which by (6.4) would have been the case for a parameter value a near the level one. The fact that the estimate of the growth rate a is significantly greater than the level one, creates a challenge for classical pricing and hedging under the fitted model. However, one can employ the generalized version of the benchmark approach with the real world pricing formula, which has been outlined in Platen (2011).

We have now determined all parameters needed for the stylized version of the model. The resulting six parameter estimates are: $A \approx 65.21$, $Y_0 \approx 1.53$, $M_0 \approx 0.0175$, $a \approx 2.55$, $\epsilon \approx 2.18$ and $\gamma \approx 265.12$. Note that we have reduced the originally eight parameters of the proposed model to six parameters, where we fixed $q = 1.0$, $\delta = 4.0$ and $\nu = 4.0$. Since the three parameters A, Y_0 and M_0 of the model are initial parameters, the model has become rather parsimonious, with only three structural parameters remaining. All three structural parameters have a clear economic meaning. The resulting model is consistent with the theoretically derived affine nature of aggregate wealth dynamics. Note that he SDE (4.3) for the normalized index in τ-time has no parameter in the drift or diffusion coefficient that has to be estimated. This means, all three parameters in the SDE (2.2) for the normalized aggregate wealth became identified as one. Therefore, we found that normalized aggregate wealth in market activity time follows most likely a very particular square root process, which is, fortunately, very tractable.

In case one restricts the dynamics of the benchmarked savings account to a process, that is a local martingale, the case that is assumed in Platen & Heath (2010), one is forced to set $a = 1$, and has only the two structural parameters ϵ and γ remaining. In this case the stylized model becomes a five parameter model with two structural parameters and three initial parameters.

8 Estimated Market Activity and Volatility

One can apply the fitted stylized model in many ways. As one possible application let us visualize for the stylized model the trajectories of the resulting market activity time and volatility, respectively. In Fig. 8.1 we show the market activity time, the τ-time, as it emerges from our estimation. One notes periods of high and low market activity generating steeper and flatter slopes, respectively, of the τ-time. The estimated τ-time is obtained directly from the observed quadratic variation of the square root of the normalized index Y when multiplied by four. One can use the modeled state variables Y_{τ_t} and $\frac{1}{M_t}$ for pricing and hedging of derivatives and for measuring and managing risk under the benchmark approach, see Platen & Heath (2010) and Platen & Bruti-Liberati (2010).

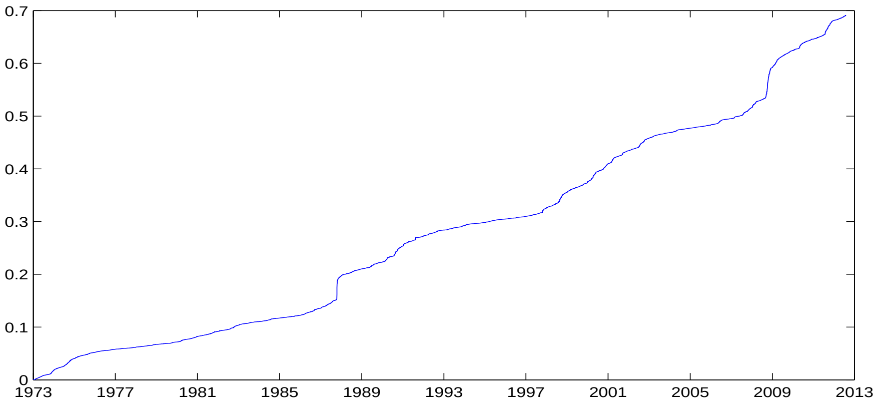

Figure 8.1: Market activity time.

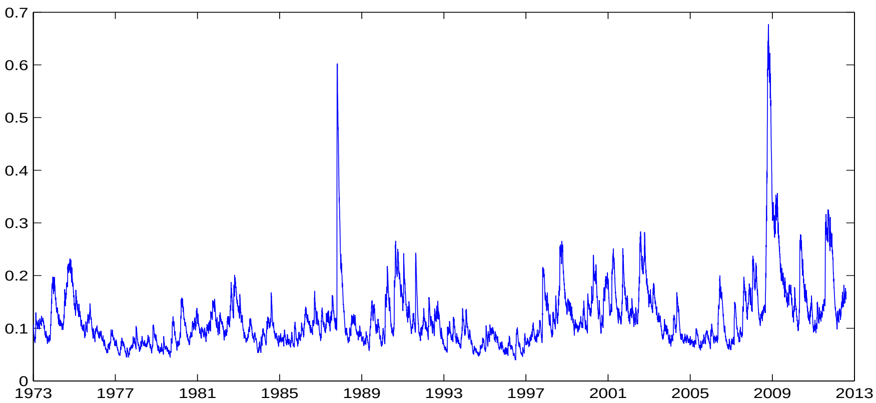

Figure 8.2: Calculated volatility of the discounted MCI for daily observations.

With the proposed model one can measure many quantities that are of interest for valuation and risk management. For instance, in recent years volatility derivatives became an important asset class. Their underlying is a volatility index of a diversified index.

For some indices the respective volatility index is available and expresses the market's view on where the (hidden) volatility may be. By formulas (5.3) and (7.2)-(7.4) the volatility of the discounted MCI equals approximately

$$\sigma_t \approx 2\sqrt{\frac{\tilde{Q}_t}{Y_{\tau_t}}}. \tag{8.1}$$

Fig. 8.2 plots the calculated volatility in t-time of the discounted MCI, obtained via formula (8.1). The volatility displayed in Fig. 8.2 is obtained from daily observations, for the period from 01/01/1973 until 10/08/2012. The sample mean of the calculated volatility in t-time equals 0.119 for the given period, which yields an estimated average volatility of about 11.9% for the MCI. This is also what one estimates from the observed log-returns of the MCI.

The proposed stylized model has been fitted by the same procedure to various diversified equity indices, including the $\mathrm{EWI114}_{40}$ constructed in Platen & Rendek (2012), the EWI104s analyzed in Le & Platen (2006) and Platen & Rendek (2008) and the MSCI world index. In each case we obtained robust results, similar to those obtained above for the MCI. By assuming that the discounted index evolution follows also in future similar dynamics with the estimated constant parameters, one obtains a probabilistic description for the future dynamics of the discounted index. Additionally, one can calibrate the model to observed index derivative prices and obtains in this case a reflection of the market's view on the future evolution of the index and its volatility.

To demonstrate along these lines that the proposed stylized model and fitting procedure applies well, even to some regional index and its options, we report in the next section results for the S&P500, where we compare the calculated volatility with the VIX, the volatility index of the S&P500.

9 Modeling the S&P500 and its Volatility Index VIX

Let us now study the case of an important regional market capitalization weighted equity index, the discounted S&P500. We consider the same time period from 01/01/1973 until 10/08/2012.

Fig. 9.1 plots the logarithm of the discounted S&P500 together with a linearly regressed trendline in calendar t-time, yielding the straight line $3.95 + 0.0378t$. This straight line provides the estimate for the parameter A with a value of about $A \approx 52.09$ and the estimated net growth rate in t-time at about a level of $\frac{4\epsilon a}{\gamma(\nu-2)} \approx 0.0378$, see (7.1). The normalized S&P500 is then obtained by dividing the discounted S&P500 by the exponential function $A_{\tau_t} \approx 52.09 \exp\{0.0378t\}$, for $t \geq 0$. Using the proposed stylized model, the resulting normalized S&P500, denoted by Y_{τ_t}, is plotted in Fig. 9.2 with respect to calendar t-time, where we set $Y_0 = 2.27$.

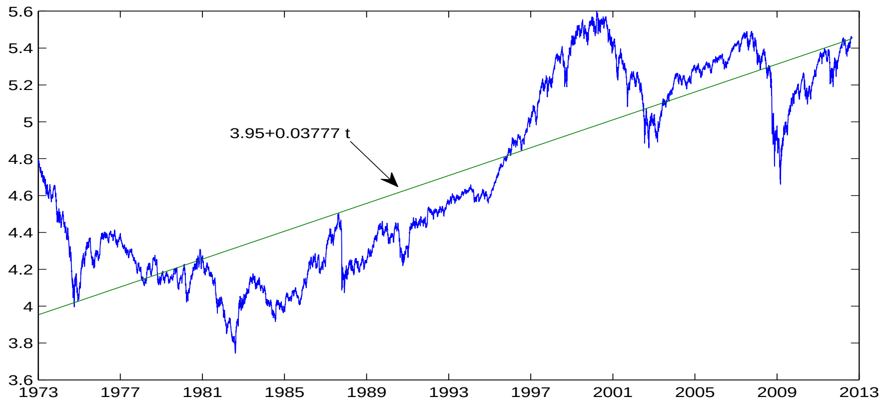

Figure 9.1: Logarithm of the discounted S&P500 and linear fit.

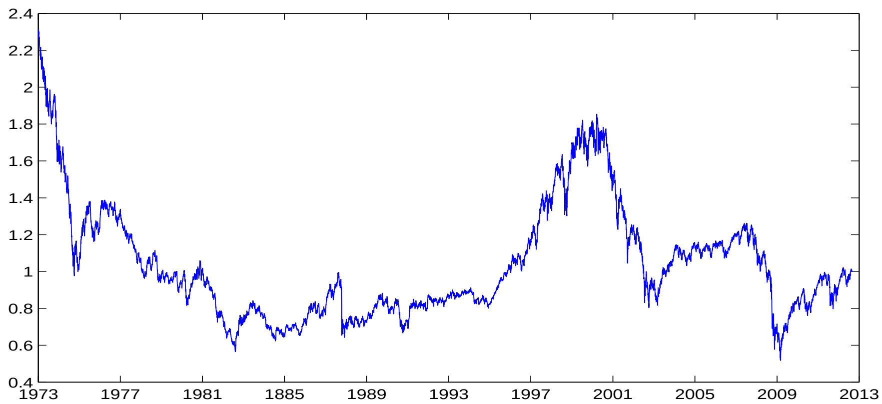

Figure 9.2: Normalized S&P500.

Fig. 9.3 plots the estimated market activity process M obtained from the normalized discounted S&P500 with daily observations shown for the period from 1973 until 2012. The process M was obtained by the same steps and using the same weight parameter $\alpha = 0.92$ for exponential smoothing, as in the case of the MCI. From the trajectory of the estimated market activity process M we obtain $\epsilon \approx 2.15$, $\gamma \approx 172.3$ and consequently $a \approx 1.5$. Note that in this case the Assumption 6.2 is approximately satisfied, and one may use in relation (6.4) the equality sign. This means, the benchmark approach, as described in Platen & Heath (2010), is potentially applicable for the S&P500 as proxy of the NP of the US market, and the stylized model employs then only five parameters.

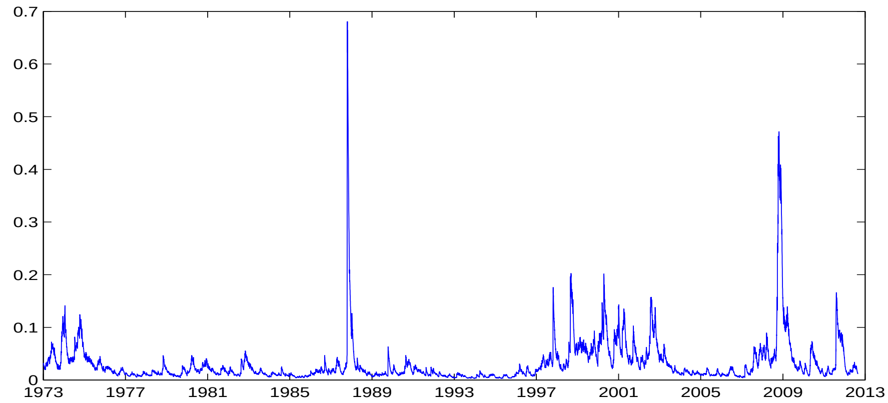

Figure 9.3: Estimated market activity process M for the S&P500 from daily data.

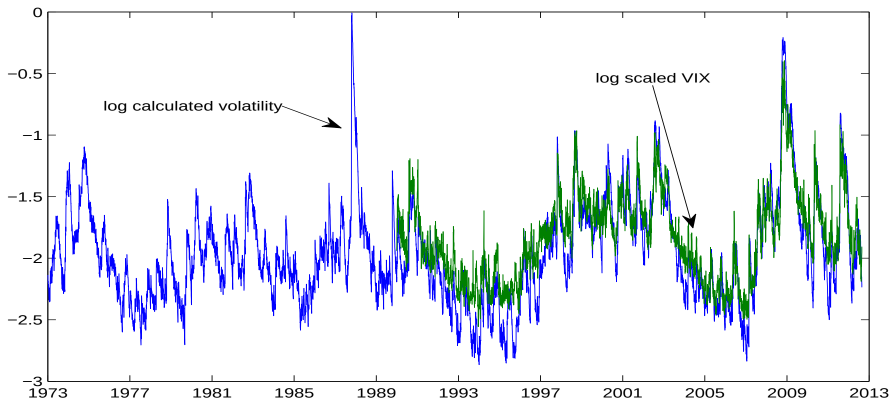

Figure 9.4: Logarithms of scaled VIX and calculated volatility of the discounted S&P500.

The volatility index VIX is provided by the Chicago Board Options Exchange. It is the volatility index for the S&P500. The literature points out that the VIX is a biased estimator of the volatility implied from index options, see e.g. Fleming, Ostdiek & Whaley (1995). Hence, it is common to match the short term at the money implied volatility by scaling the VIX. Typically, the VIX, which stems from daily observations, is known to multiply the implied volatility by a factor of about 1.2; see e.g. Blair, Poon & Taylor (2001). That is, when denoting by VIX_t the value of the quoted VIX at time t, then one obtains the scaled VIX value V_t via the formula

$$V_t = \frac{\mathrm{VIX}_t}{100} \frac{1}{1.2}, \tag{9.1}$$

for $t \geq 0$, which provides approximately the at the money implied volatility of short term S&P500 options.

Fig. 9.4 plots the calculated volatility in calendar t-time of the discounted S&P500,

calculated according to formula (8.1), and obtained from daily observations, for the period from 02/01/1990 until 10/08/2012. The sample mean of the calculated volatility in t-time equals 0.1625 for the given period. For comparison, the daily data for the logarithm of the scaled VIX, according to (9.1), are also shown in Fig. 9.4. The sample mean of the scaled VIX is with 0.1707 close to that of the calculated volatility. The logarithm of the scaled VIX behaves in Fig. 9.4 very similarly to the logarithm of the calculated volatility of the discounted S&P500, obtained under the proposed stylized model. To generate the volatility, the proposed model combines in formula (5.3) the normalized discounted S&P500, modeled by Y_{τ_t} and displayed in Fig. 9.2 with the market activity process M, displayed in Fig. 9.3. As one can see, via formula (5.3) the proposed model recovers visually with good accuracy the trajectory of the scaled VIX from the trajectories of the two observable processes Y_{τ_t} and M_t. We emphasize that the proposed stylized model is parsimonious by construction and uses only two constant structural parameters for its characterization. These parameters seem to remain the same also over long periods of time. Furthermore, the model employs only one Brownian motion, which makes it a one-factor model with two state variables.

Since calculated volatility recovers the VIX accurately it can be expected to recover also well short dated, close to at the money European option prices on the S&P500 index.

10 Simulation Study

This section explains the steps we propose for the simulation of the stylized version of the model. Both square root processes $\frac{1}{M}$ and Y are simulated jointly by sampling from their non-central chi-square transition density with the same sources of randomness, see also Platen & Rendek (2009) or Platen & Bruti-Liberati (2010). We will see that this simulation is performed without any error for $\frac{1}{M}$ and almost exactly for Y.

The following illustration of the simulation of the stylized version of the model uses the six parameter values estimated in Section 7 for the MCI. The simulation is performed using the following steps:

1. Simulation of the Process $\frac{1}{M}$

The inverse $\frac{1}{M}$ of the market activity process we have to simulate first. It is described by the SDE (4.8) and is a square root process of dimension $\nu = 4$.

This process can be sampled exactly due to its non-central chi-square transition density of dimension $\nu = 4$. That is, we have

$$\frac{1}{M_{t_{i+1}}} = \frac{\gamma(1-e^{-\epsilon(t_{i+1}-t_i)})}{4\epsilon}\left(\chi^2_{3,i} + \left(\sqrt{\frac{4\epsilon e^{-\epsilon(t_{i+1}-t_i)}}{\gamma(1-e^{-\epsilon(t_{i+1}-t_i)})}\frac{1}{M_{t_i}}} + Z_i\right)^2\right), \quad (10.1)$$

for $t_i = \Delta i, i \in \{0, 1, \ldots\}$; see also Broadie & Kaya (2006). Here Z_i is an independent standard Gaussian distributed random variable and $\chi^2_{3,i}$ is an independent chi-square distributed random variable with three degrees of freedom. Then the right hand side of (10.1) becomes a non-central chi-square distributed random variable with the requested non-centrality and four degrees of freedom.

A simulated path of M_{t_i}, according to (10.1), is displayed in Fig. 10.1 for a period of 40 years using the previously estimated parameters for the MCI. It resembles the type of trajectory shown in Fig. 7.3 with more pronounced spikes than those observed in Fig. 7.3 that were caused by the 1987 crash and the GFC in 2007/2008. We will see later that the estimated market activity obtained from the simulated index resembles strongly the estimated trajectory of the market activity of the MCI, displayed in Fig. 7.3, which showed less peaked spikes.

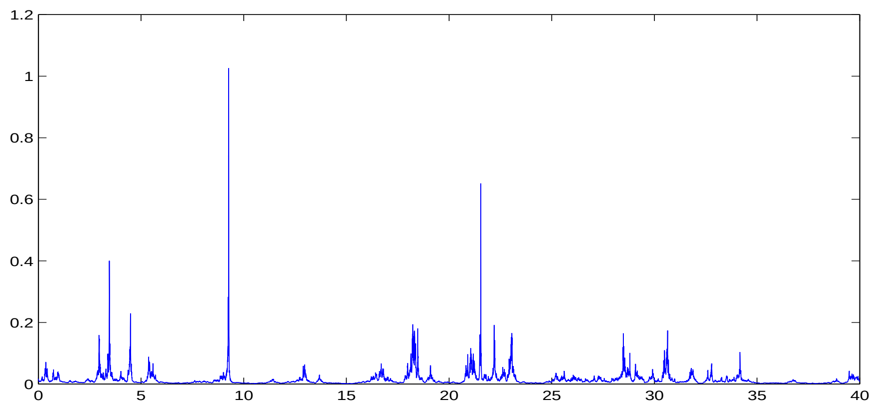

Figure 10.1: Simulated path of M.

2. Calculation of τ-Time

The next step of the simulation generates the market activity time, the τ-time. By (4.7) one aims for the increment

$$\tau_{t_{i+1}} - \tau_{t_i} = \int_{t_i}^{t_{i+1}} M_s ds, \quad (10.2)$$

$i \in \{0, 1, \ldots\}$. To avoid any anticipation of future uncertainty the integral on the right hand side of equation (10.2) is numerically approximated by the product

$$M_{t_i}(t_{i+1} - t_i). \quad (10.3)$$

Fig. 10.2 displays the resulting τ-time, the market activity time, which resembles well that shown in Fig. 8.1.

3. Calculation of the Y Process

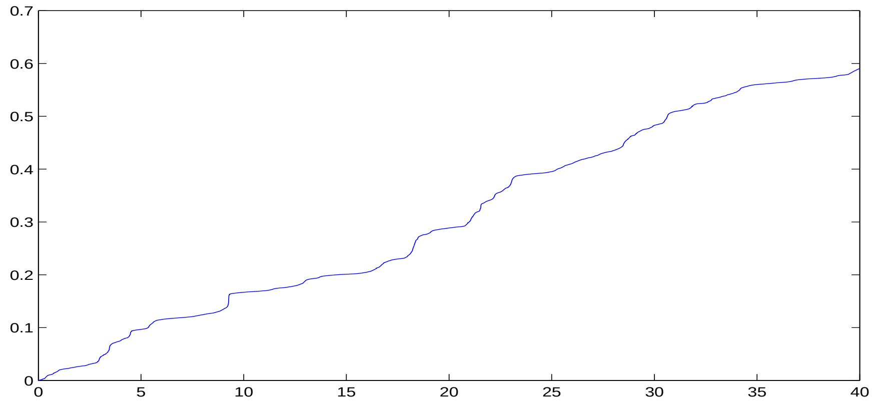

Figure 10.2: Simulated τ-time, the market activity time.

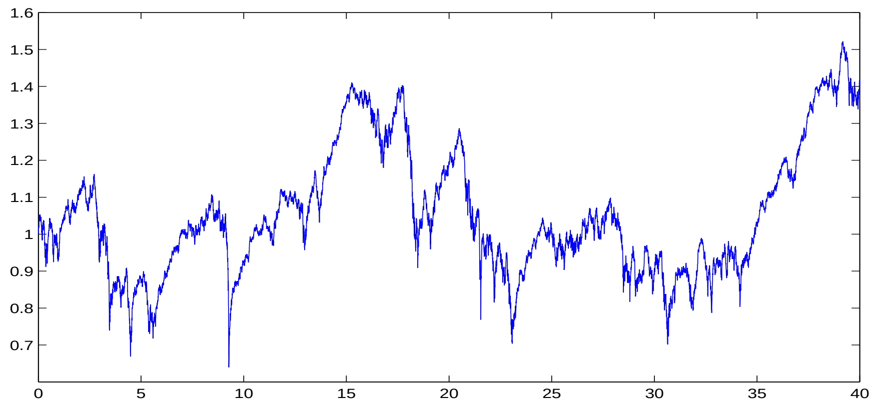

Figure 10.3: Simulated trajectory of the normalized index Y_{τ_t}.

The simulation of the Y process is very similar to the simulation of the square root process $\frac{1}{M}$. Both processes are square root processes of dimension four and both are driven by the same source of uncertainty. We therefore employ in each time step the same Gaussian random variable Z_i and the same chi-square distributed random variable $\chi^2_{3,i}$, as in (10.1), to obtain the new value of the Y process,

$$Y_{\tau_{t_{i+1}}} = \frac{1 - e^{-(\tau_{t_{i+1}} - \tau_{t_i})}}{4} \left(\chi^2_{3,i} + \left(\sqrt{\frac{4e^{-(\tau_{t_{i+1}} - \tau_{t_i})}}{1 - e^{-(\tau_{t_{i+1}} - \tau_{t_i})}} Y_{\tau_{t_i}}} + Z_i \right)^2 \right), \qquad (10.4)$$

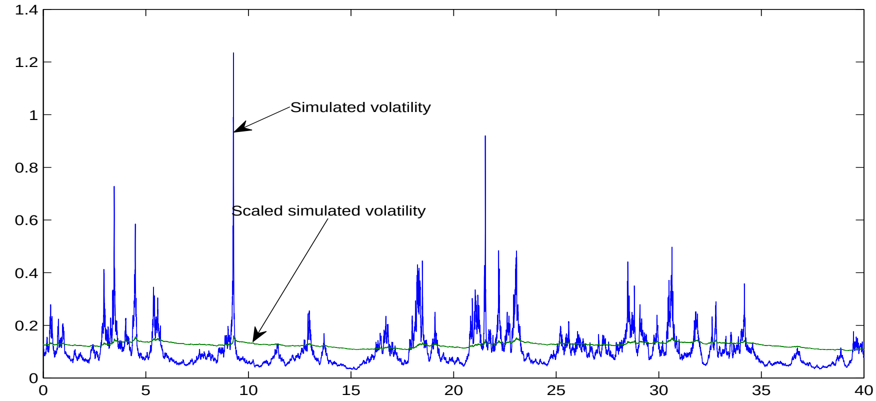

Figure 10.4: Simulated volatility of the index and simulated scaled volatility.

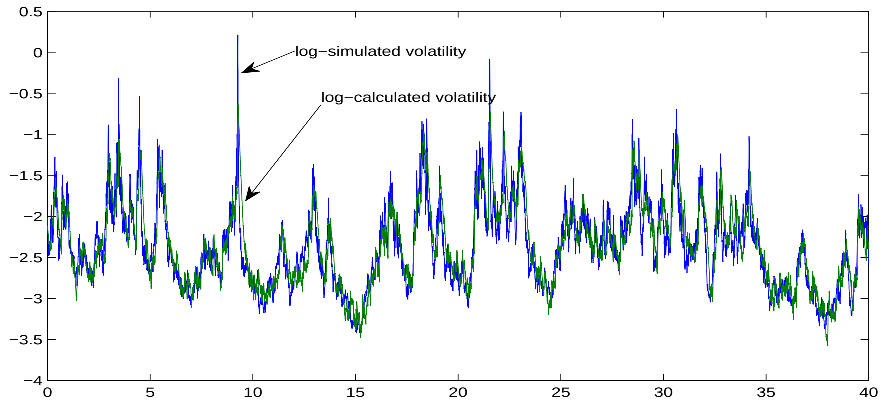

Figure 10.5: Logarithm of the simulated and calculated volatility.

for $t_i = \Delta i, i \in \{0, 1, \dots\}$. Note that the difference $\tau_{t_{i+1}} - \tau_{t_i}$ was approximated using in (10.3) the market activity of the previous step. For small step size the approximation of (10.2) by (10.3) is rather accurate and we say that Y_{τ_t} is here almost exactly simulated. This is significantly better in accuracy over long time periods than what discrete time approximations, in the sense of Kloeden & Platen (1999), can deliver.

For simplicity, we choose in the simulation the initial value $Y_0 = 1$. The resulting trajectory of the normalized index process Y is exhibited in Fig. 10.3, which shows strong similarity with Fig. 7.2. Interesting is that one observes from time to time major sharp drawdowns in the simulated path. The accurate modeling of such drawdowns is crucial for risk measurement.

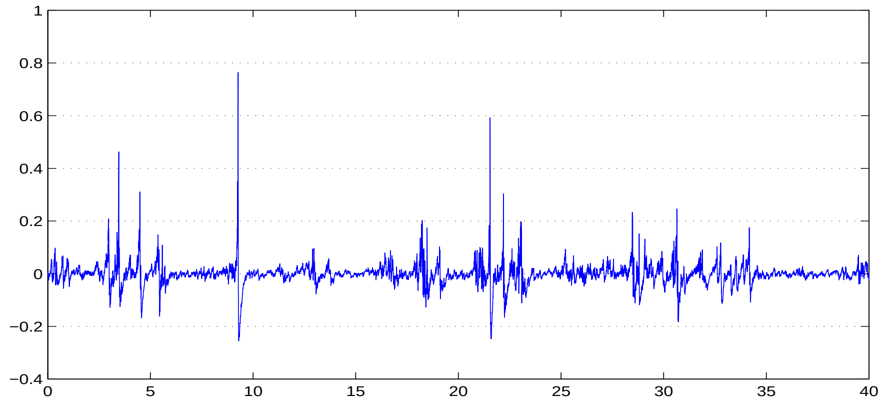

Figure 10.6: Differences of the logarithms of the simulated and calculated volatility.

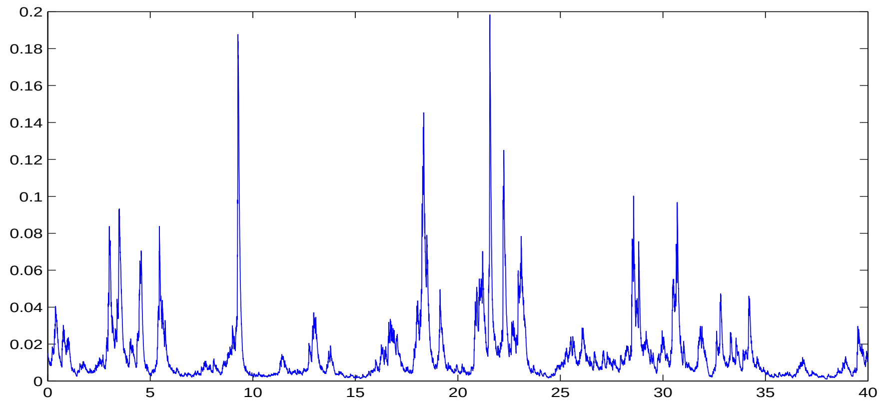

Figure 10.7: Estimated market activity of the simulated index.

4. Calculating the Volatility Process

One obtains the trajectory of the simulated volatility σ_t of the index by formula (5.3). The resulting simulated trajectory of the volatility is displayed in Fig. 10.4. For comparison, the same figure shows also the simulated "scaled volatility" given by the formula $\sqrt{\frac{2\epsilon}{\gamma Y_{\tau_t}}}$, which is the volatility resulting purely from the feedback mechanism of the market with respect to "average" τ-time. One notes that the simulated volatility deviates significantly from the "scaled simulated volatility". One notes in the simulated volatility the "exaggerated" values above and below the "scaled simulated volatility". This deviation is modeling the way how market activity is evolving. It models overreactions (underreactions) in response to each downward (upward) move of the index.

For comparison, Fig. 10.5 shows the logarithm of the simulated volatility displayed

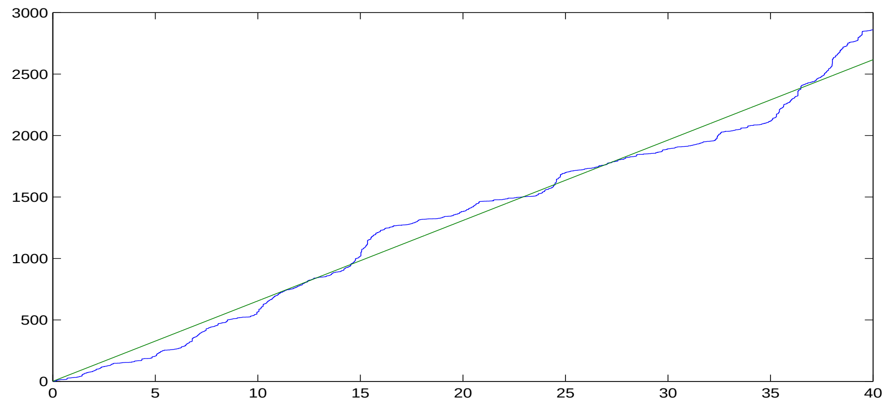

Figure 10.8: Quadratic variation of the square root of the inverse of estimated market activity.

in Fig. 10.4 together with the logarithm of the calculated volatility according to formula (8.1) by using the estimated market activity, which is first calculating $\tilde{Q}$ from (7.3) and (7.4). These trajectories are visually similar but not identical. The calculated volatility is smoother and lagging behind since it results from the smoothing we use to obtain the estimated market activity process. Additionally, in Fig. 10.6 we show the differences between the logarithms of the simulated and calculated volatility.

Fig. 10.7 shows the estimated market activity from the simulated index. We see that the extreme spikes of the simulated M in Fig. 10.1 are substantially smoothed in the estimated market activity shown in Fig. 10.7. Fig. 10.7 resembles well the estimated market activity of the MCI in Fig. 7.3. Moreover, we calculate the quadratic variation of the square root of the inverse of the estimated market activity from the simulated index and plot it in Fig. 10.8. Note the strong similarity of this figure to Fig. 7.4. It is important to take the effects of the smoothing into account when interpreting the dynamics of the index and these of the observed quantities.

The above simulation has shown that the proposed stylized model generates trajectories with visually very similar properties as observed from the MCI. The next section will confirm that all listed stylized empirical facts, which are typical for most diversified stock indices, are captured by the stylized model.

11 Empirical Properties of the Proposed Model

For the proposed stylized model this section checks the seven stylized empirical facts, listed in Section 3. We will see whether its properties would allow one to falsify the model. We employ the same standard statistical and econometric

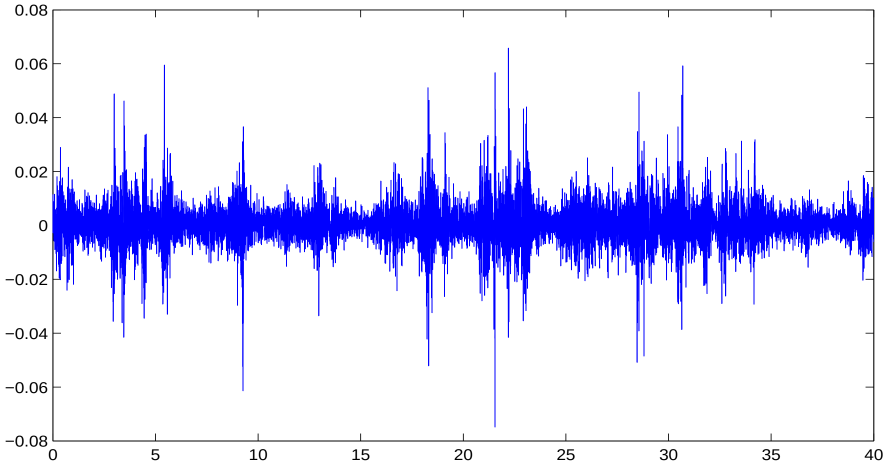

Figure 11.1: Log-returns of the simulated index.

techniques as used in Section 3. The daily observed index is simulated, as described in the previous section, using the estimated parameters for the MCI. The trajectories we display in this section correspond to the trajectories exhibited in the figures in Section 10. Fig. 11.1 displays the daily log-returns of the simulated index, these resemble visually well those of Fig. 3.2.

(i) Uncorrelated Returns

Daily observed simulations of the equity index under the proposed model provide typical graphs of the Y process similar to those shown in Fig. 10.3. As one should expect, due to the construction of the model there is practically no correlation detectable between the log-returns over time. Fig. 11.2 displays the average over 26 estimated autocorrelation functions for log-returns of the simulated index, which rapidly falls to the level zero with more than 95% significance, similarly as observed in Fig. 3.3.

(ii) Correlated Absolute Returns

In a similar manner also the average autocorrelation for the absolute log-returns of the simulated index has been estimated. In Fig.11.3 the average of 26 estimated autocorrelation functions of absolute log-returns is displayed. Similarly, as in Fig. 3.4, one observes that this average of sample autocorrelations does not die away fast. Moreover, as in Fig. 3.4, the decay of the autocorrelation does not seem to be exponential. Even for large lags of more than one month there is still some significant autocorrelation present.

(iii) Student-t Distributed Returns

By the same maximum likelihood estimation method as employed earlier we analyzed 40 years of daily log-returns of the simulated index. As expected

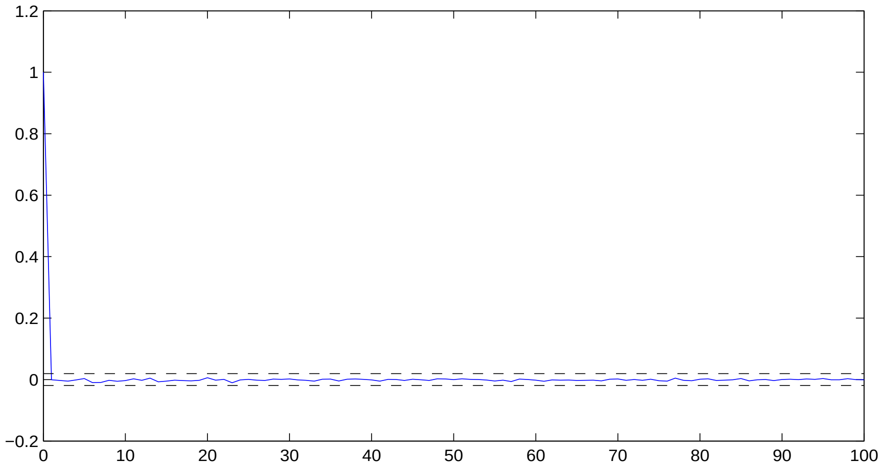

Figure 11.2: Average autocorrelation function for log-returns of the simulated index.

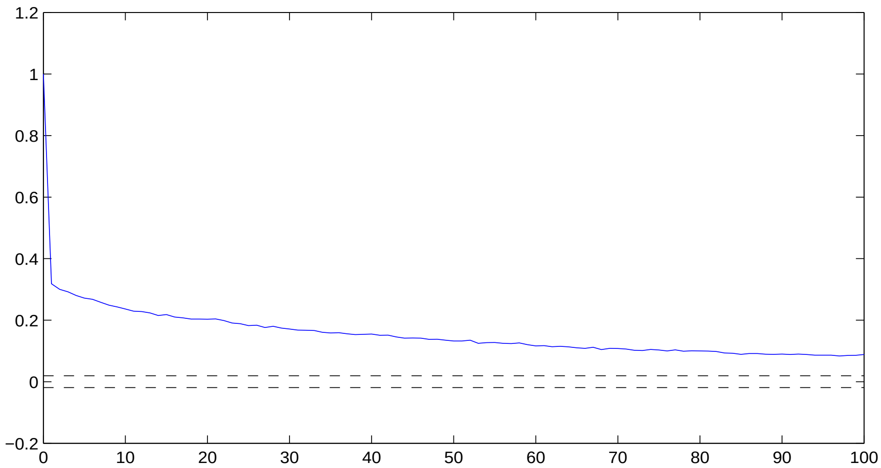

Figure 11.3: Average autocorrelation function for the absolute log-returns of the simulated index.

from the design of the model these appear to be distributed according to a Student-t distribution with approximately four degrees of freedom. Fig. 11.4 displays the logarithm of the empirical density of simulated normalized index returns displayed in Fig. 11.1. This figure shows also the logarithm of the density of the Student-t distribution, which in this case was estimated with 3.2 degrees of freedom. The fit to the simulated data seems visually similarly good as in Fig. 3.5. Note that even though the simulation was performed with $\delta = 4$ the estimated degrees of freedom of the Student-t density fitted to the simulated data can easily be almost one degree different

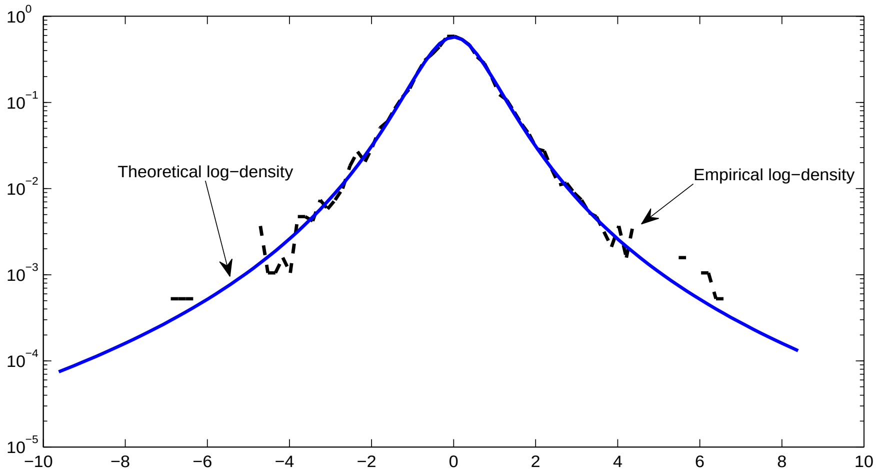

Figure 11.4: Logarithm of empirical density of normalized log-returns of the simulated index and Student-t density with 3.2 degrees of freedom.

Table 11.3: Log-Maximum likelihood test statistic for different outcomes of the simulated normalized log-returns

Simulation	Student-t	NIG	Hyperbolic	VG	ν
1	0.008934	37.474149	102.719638	131.240780	4.012850
2	11.485226	11.175028	96.457136	132.916256	3.450916
3	0.000000	100.928524	244.190151	294.719960	3.734148
4	9.002421	35.759464	347.060676	331.014904	2.579009
5	8.767003	11.551178	121.190482	144.084964	3.170449
6	0.401429	60.570898	205.788160	252.591737	3.432435
7	12.239056	4.354888	46.411554	78.273485	3.957696
8	1.693411	23.910523	94.408789	130.623174	3.849691
9	1.232454	47.830407	202.073144	237.168411	3.236322
10	0.000000	43.037206	128.807757	162.582353	3.774957
11	0.433645	47.782681	172.736397	208.847632	3.431803
12	0.000000	56.019354	146.077121	185.624888	3.899403
13	7.137154	48.219756	579.922931	477.383441	2.293363
14	5.873948	16.515390	107.770531	135.508299	3.388307
15	0.000000	54.718046	184.112794	217.304105	3.402049
16	6.982560	3.991610	29.192198	47.105125	4.268740
17	2.966916	22.914863	108.513143	138.044416	3.553629
18	0.000000	52.066364	129.790856	160.373085	3.959605
19	0.006909	39.568695	111.398645	143.914350	3.982892
20	0.000001	56.845664	169.915512	211.260626	3.651091
21	1.674578	17.681088	61.710576	90.679738	4.265834
22	14.010840	3.279722	47.433693	73.789313	3.770825
23	11.198940	12.074044	114.888817	143.800553	3.257146
24	0.455557	27.676102	86.841704	114.452947	4.006528
25	6.658059	13.403411	90.314637	119.523602	3.502497
26	19.812830	1.360441	37.443467	59.435233	3.821602

as in Fig. 11.4.

Additionally, Table 11.3 provides, similarly to Table 3.2, the test statistics for the Student-t fit and several other symmetric generalized hyperbolic distributions for 26 cases of 40 years simulated log-returns. We note that our estimation provided in many simulations less than four degrees of freedom. This means that there is variation in the estimation of the degrees of freedom and the stylized model based on the theoretical understanding of aggregate wealth dynamics cannot be easily falsified on this ground.

(iv) Volatility Clustering

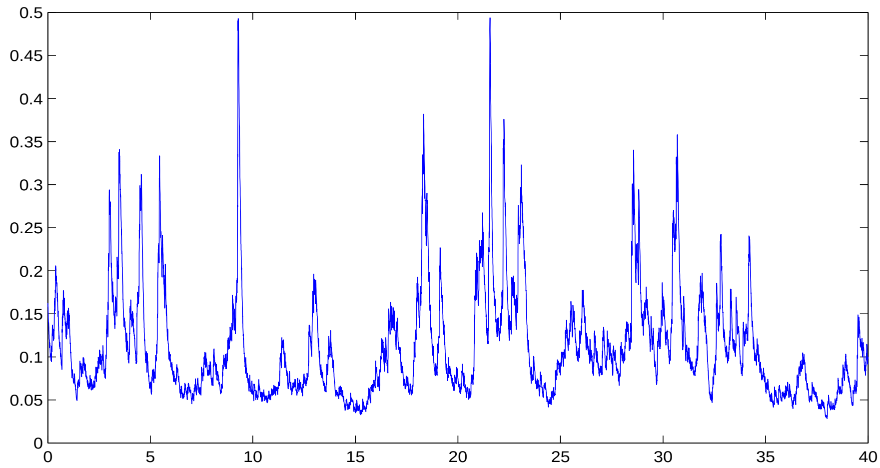

Figure 11.5: Estimated volatility of the simulated index.

Obviously, under the proposed model volatility is stochastic. A moving average estimation of volatility from the simulated index log-returns results in the volatility shown in Fig. 11.5. One clearly notes that this observed volatility is indeed stochastic, and it shows clusters of higher values for certain random time periods of time. Note that the graph in Fig. 11.5 is not exactly the volatility that we can calculate under the model, because it is estimated as a standard moving average from the index log-returns. The logarithm of the via moving average estimated volatility is displayed in Fig. 11.7.

The proposed model agrees with the stylized empirical fact (iv), which expresses the growing consensus among practitioners and academic researchers that volatility should be modeled as a stochastic process that generates occasional outbursts of volatility clusters. Note that, in reality, one cannot fully observe the hidden exact volatility. Fig. 10.6 illustrates the potential difference between the simulated volatility and our calculated volatility. In Fig. 11.8 we show the differences between the logarithm of the simulated and the estimated volatility from squared index log-returns. When comparing Fig. 10.6 and Fig. 11.8 one notes that the calculated volatility, we propose in Section 7 is, in general, closer to the simulated volatility.

(v) Long Term Exponential Growth

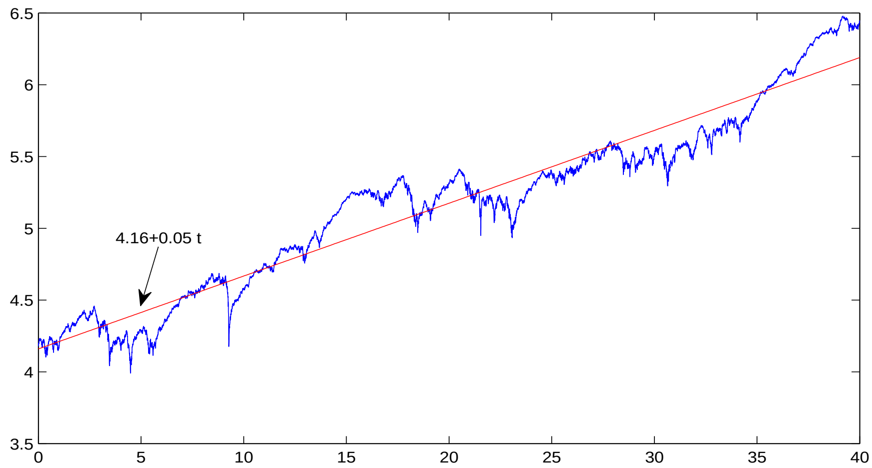

Figure 11.6: Logarithm of simulated index with linear fit.

In Fig. 11.6 the logarithm of the simulated index has been displayed with its fit to a straight line. Here the linear regression of the logarithm of the simulated index provided the estimates with $A = 64.07$, $\frac{2a\epsilon}{\gamma} = 0.05$.

The logarithm of the simulated normalized index, $\ln(Y)$, is displayed as upper graph in Fig. 11.7. As requested, Y has a stationary density by construction.

(vi) Leverage Effect

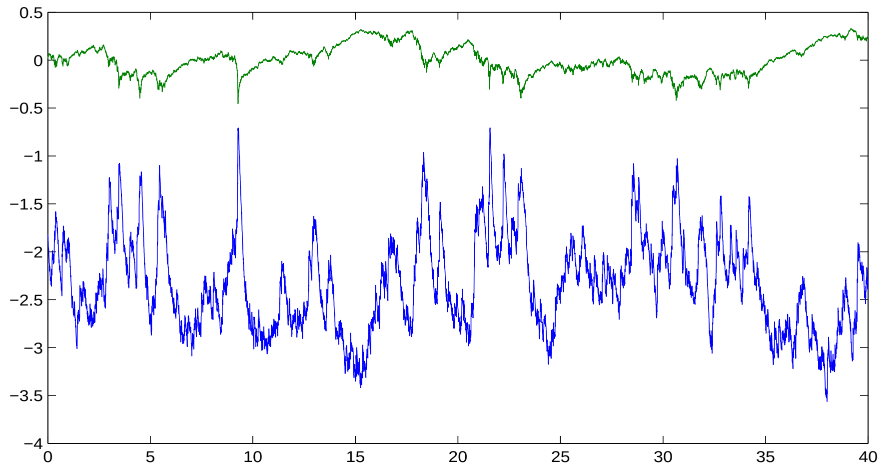

Figure 11.7: Logarithms of simulated normalized index and its estimated volatility.

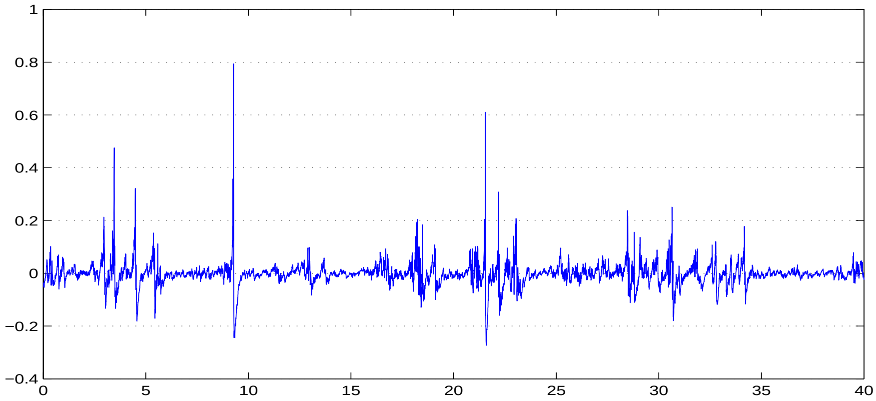

Figure 11.8: Differences of the logarithms of the simulated and estimated volatility.

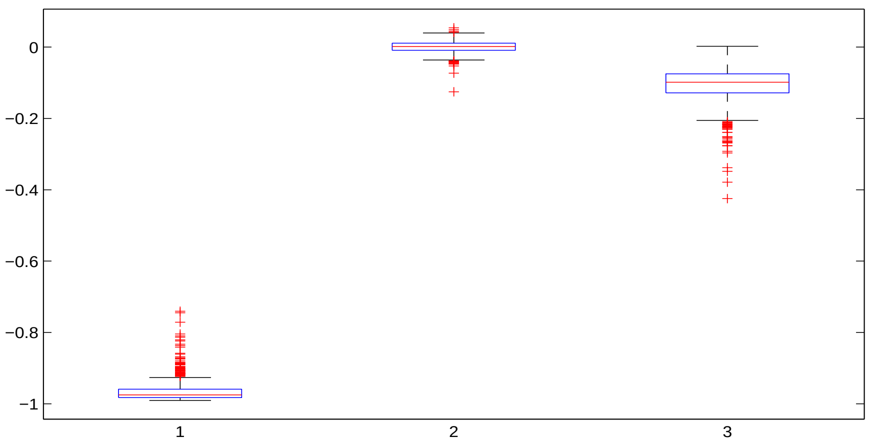

Figure 11.9: Boxplots of correlation coefficient obtained by methods 1-3.

Fig. 11.7 is plotting the logarithm of the simulated normalized index together with the logarithm of its via standard moving average from squared log-returns estimated volatility. By construction, under the proposed model the simulated volatility, as given in formula (5.3), of the simulated index is perfectly negatively "dependent" on the normalized index. We pointed already out that our calculated volatility lags slightly behind the simulated volatility, as shown in Fig. 10.5.

Let us now perform the following study: We simulate 1000 trajectories of the index and its volatilities and calculate the correlation coefficient between the increments of the logarithm of the simulated index and the increments of the logarithms of the three types of volatilities. These volatilities are obtained by the following three methods:

1. The simulated volatility is obtained from the proposed model by first simulating the market activity process M and then the normalized index Y. The volatility is then obtained via formula (5.3).
2. The estimated volatility is obtained from exponential smoothing of squared index log-returns via a moving average.
3. The calculated volatility is obtained from formula (8.1) by first calculating $\tilde{Q}$ from (7.3) and (7.4).

Fig. 11.9 shows the boxplots corresponding to the correlation coefficient obtained for the volatilities calculated by the three methods. It is clear that the correlation coefficient depends clearly on the method used for the calculation of the volatility even that graphs appear to be visually very similar. We observe on average $-0.9656(-0.9679, -0.9632)$, $0.000605(-0.000645, 0.0019)$ and $-0.1073(-0.1112, -0.1035)$ of correlation (with the 99% confidence interval shown in the brackets) between the increments of the logarithm of the simulated index and increments of the logarithm of the volatility obtained by the methods 1-3, respectively. This important effect has been pointed out in the work by Ait-Sahalia, Fan & Li (2012). We argue in this paper that there is no need to introduce an extra independent Brownian motion as driver of stochastic volatility of a diversified index even if one does not observe perfect negative correlation between log-returns and estimated volatility increments.

(vii) Extreme Volatility at Major Downward Moves

In Fig. 11.7 one observes that the logarithm of the volatility increases more than the logarithm of the simulated index moves down at major downward moves of the index. In periods of "normal" index fluctuations the magnitudes of their movements have been more in line. This means, in times of crisis the increase of the volatility is stronger under the proposed model than could be typically generated by, say, a local volatility function model. The proposed more complex interplay between market activity and index fluctuations reflects well the extreme volatilities at major downward moves observed in the market.

In summary, one can say that the proposed model captures well and safely all seven stylized empirical facts listed in Section 3 and cannot be falsified on these grounds. This list of properties was also sufficient to identify the proposed stylized model as a two component diffusion model with six parameters.

There is significant potential to generalize the proposed model so that it can potentially match even better reality. Most obvious is the possible inclusion of jumps in market activity triggered by major drawdowns of the index. Furthermore, one could use a local volatility function in the process Y to give flexibility to the implied volatility surface of index options. Finally, one could make some of the parameters time dependent or even regime switching stochastic. However, it is questionable whether the available data are sufficient to falsify the stylized model with constant parameters when compared with such generalizations.

References

Ait-Sahalia, Y., J. Fan, & Y. Li (2012). The leverage effect puzzle: Disentangling sources of bias at high frequency. *Working Paper*.

Alfonsi, A. (2005). On the discretization schemes for the CIR (and Bessel squared) processes. *Monte Carlo Methods Appl.* **11**(4), 355–384.

Alparslan, A., A. Tessitore, & N. Usmen (2012). Stable Paretian vs. Student's t stock market hypothesis. *(Working Paper)*.

Ané, T. & H. Geman (2000). Order flow, transaction clock and normality of asset returns. *J. Finance* **60**(5), 2259–2284.

Barndorff-Nielsen, O. (1977). Exponentially decreasing distributions for the logarithm of particle size. *Proceedings of the Royal Society of London, Series A* **353**, 401–419.

Barndorff-Nielsen, O. (1997). Normal inverse Gaussian distributions and stochastic volatility modelling. *Scand. J. Statist.* **24**, 1–13.

Barndorff-Nielsen, O. & N. Shephard (2001). Modelling by Lévy processes for financial econometrics. In O. E. Barndorff-Nielsen, T. Mikosch, and S. Resnick (Eds.), *Lévy Processes - Theory and Applications*, pp. 283–318. Birkhäuser, Boston.

Black, F. (1976). Studies in stock price volatility changes. In *Proceedings of the 1976 Business Meeting of the Business and Economic Statistics Section, American Statistical Association*, pp. 177–181.

Black, F. & M. Scholes (1973). The pricing of options and corporate liabilities. *J. Political Economy* **81**, 637–654.

Blair, B. J., S. Poon, & S. Taylor (2001). Forcasting S&P 100 volatility: The incremental information content of implied volatilities and high frequency index returns. *Journal of Econometrics* **105**(1), 5–26.

Bochner, S. (1955). *Harmonic Analysis and the Theory of Probability.* University of California Press, Berkeley, CA.

Broadie, M. & O. Kaya (2006). Exact simulation of stochastic volatility and other affine jump diffusion processes. *Oper. Res.* **54**, 217–231.

Carr, P., H. Geman, D. Madan, & M. Yor (2004). From local volatility to local Lévy models. *Quant. Finance.* **4**, 581–588.

Carr, P. & J. Sun (2007). A new approach for option pricing under stochastic volatility. *Rev. Deriv. Research* **10**, 87–150.

Clark, P. K. (1973). A subordinated stochastic process model with finite variance for speculative prices. *Econometrica* **41**, 135–159.

Cont, R. (2010). *Encyclopedia of Quantitative Finance*. Wiley.

Cox, J. C. (1975). Notes on option pricing I: constant elasticity of variance diffusions. Stanford University, (working paper, unpublished).

Cox, J. C., J. E. Ingersoll, & S. A. Ross (1985). A theory of the term structure of interest rates. *Econometrica* **53**, 385–407.

Cox, J. C. & S. A. Ross (1976). The valuation of options for alternative stochastic processes. *J. Financial Economics* **3**, 145–166.

Delbaen, F. & W. Schachermayer (1994). A general version of the fundamental theorem of asset pricing. *Math. Ann.* **300**, 463–520.

Derman, E. & I. Kani (1994a). Riding on a smile. *Risk* **7**, 32–39.

Derman, E. & I. Kani (1994b). The volatility smile and its implied tree. *Goldman Sachs Quantitative Strategies Research Notes*.

Diop, A. (2003). *Sur la discrétisation et le comportement á petit bruit d'EDS multidimensionnalles dont les coefficients sont á dérivées singuliéres*. Ph. D. thesis, INRIA.

Duffie, D. & R. Kan (1994). Multi-factor term structure models. *Philos. Trans. Roy. Soc. London Ser.* A **347**, 577–580.

Dupire, B. (1992). Arbitrage pricing with stochastic volatility. In *Proceedings of AFFI Conference, Paris*.

Dupire, B. (1993). Model art. *Risk* **6**, 118–124.

Eberlein, E. & U. Keller (1995). Hyperbolic distributions in finance. *Bernoulli* **1**, 281–299.

Engle, R. F. (1982). Autoregressive conditional heteroskedasticity with estimates of the variance of U.K. inflation. *Econometrica* **50**(4), 987–1007.

Fergusson, K. & E. Platen (2006). On the distributional characterization of log-returns of a world stock index. *Appl. Math. Finance* **13**(1), 19–38.

Fleming, J., B. Ostdiek, & R. E. Whaley (1995). Predicting stock market volatility: a new measure. *Journal of Futures Markets* **15**, 265–302.

Ghysels, E., A. Harvey, & E. Renault (1996). Stochastic volatility. In *Statistical Methods in Finance*, Volume 14 of *Handbook of Statist.*, pp. 119–191. North-Holland.

Hagan, P. S., D. Kumar, A. S. Lesniewski, & D. Woodward (2002). Managing smile risk. *Willmot*, 84–108.

Harrison, J. M. & D. M. Kreps (1979). Martingale and arbitrage in multiperiod securities markets. *J. Economic Theory* **20**, 381–408.

Heston, S. L. (1993). A closed-form solution for options with stochastic volatility with applications to bond and currency options. *Rev. Financial Studies* **6**(2), 327–343.

Hurst, S. R. & E. Platen (1997). The marginal distributions of returns and volatility. In Y. Dodge (Ed.), L_1*-Statistical Procedures and Related Topics*, Volume 31 of *IMS Lecture Notes - Monograph Series*, pp. 301–314. Institute of Mathematical Statistics Hayward, California.

Kahneman, D. & A. Tversky (1979). Prospect theory: an analysis of decision under risk. *Econometrica* **47**(2), 263–292.

Kloeden, P. E. & E. Platen (1999). *Numerical Solution of Stochastic Differential Equations*, Volume 23 of *Appl. Math.* Springer. Third printing, (first edition (1992)).

Kou, S. G. (2002). A jump diffusion model for option pricing. *Management Science* **48**, 1086–1101.

Le, T. & E. Platen (2006). Approximating the growth optimal portfolio with a diversified world stock index. **7**(5), 559–574.

Lewis, A. L. (2000). *Option Valuation Under Stochastic Volatility.* Finance Press, Newport Beach.

Loewenstein, M. & G. A. Willard (2000). Local martingales, arbitrage, and viability: Free snacks and cheap thrills. *Econometric Theory* **16**(1), 135–161.

Long, J. B. (1990). The numeraire portfolio. *J. Financial Economics* **26**, 29–69.

Madan, D. & E. Seneta (1990). The variance gamma (V.G.) model for share market returns. *J. Business* **63**, 511–524.

Markowitz, H. & N. Usmen (1996a). The likelihood of various stock market return distributions, Part 1: Principles of inference. *J. Risk & Uncertainty* **13**(3), 207–219.

Markowitz, H. & N. Usmen (1996b). The likelihood of various stock market return distributions, Part 2: Empirical results. *J. Risk & Uncertainty* **13**(3), 221–247.

McNeil, A., R. Frey, & P. Embrechts (2005). *Quantitative Risk Management.* Princeton University Press.

Mehra, R. & E. C. Prescott (1985). The equity premium: A puzzle. *J. Monetary Economy* **15**, 145–161.

Merton, R. C. (1973). An intertemporal capital asset pricing model. *Econometrica* **41**, 867–888.

Platen, E. (1997). A non-linear stochastic volatility model. Technical report, Australian National University, Canberra, Financial Mathematics Research Reports. FMRR 005-97.

Platen, E. (2011). A benchmark approach to investing and pricing. in:. *MacLean, L.C. and Thorp, E. O. and Ziemba, W. (2011), The Kelly Capital Growth Investment Criterion. World Scientific.*, 409–425.

Platen, E. & N. Bruti-Liberati (2010). *Numerical Solution of Stochastic Differential Equations with Jumps in Finance*. Springer.

Platen, E. & D. Heath (2010). *A Benchmark Approach to Quantitative Finance*. Springer Finance. Springer.

Platen, E. & R. Rendek (2008). Empirical evidence on Student-*t* log-returns of diversified world stock indices. *Journal of Statistical Theory and Practice* **2**(2), 233–251.

Platen, E. & R. Rendek (2009). Exact scenario simulation for selected multidimensional stochastic processes. *Communications on Stochastic Analysis* **3**(3), 443–465.

Platen, E. & R. Rendek (2012). Approximating the numéraire portfolio by naive diversification. *Journal of Asset Management* **13**(1), 34–50.

Popper, K. R. (1934). *Logik der Forschung.* Springer, Vienna. Amplified English edition, Popper (1959).

Revuz, D. & M. Yor (1999). *Continuous Martingales and Brownian Motion* (3rd ed.). Springer.

Ross, S. A. (1976). The arbitrage theory of capital asset pricing. *J. Economic Theory* **13**, 341–360.

Rubinstein, M. (1976). The strong case for the generalized logarithmic utility model as the premier model of financial markets. *J. Finance* **31**, 551–571.